SUPPORTING INFORMATION

Table of Contents

Experimental Procedures

Materials. Materials were purchased from commercial vendors and used without further purification. All deuterated solvents were purchased from Cambridge Isotope Laboratories. Isoamyl nitrite was purchased from Acros Organic. Disodium ethylenediaminetetraacetate dihydrate (EDTA) was purchased from Alfa Aesar. 13(S)-HpODE, recombinant human 5-lipoxygenase, and methylamine hexamethylene methylamine NONOate (MAHMA-NONOate) was purchased from Cayman Chemicals. Sodium diethyldithiocarbamate trihydrate (DETC) was purchased from Chem-Impex Incorporated. Corning® Supersomes™ Human Monoamine Oxidase A was purchased from Corning Inc. Acetone, ammonium chloride, Mitsubishi™ AnaeroPack™-Anaero Anaerobic gas generator, bovine serum albumin (lyophilized), dichloromethane, dimethyl sulfoxide, glacial acetic acid, oxalyl chloride (Acros), phosphate saline buffer (Corning), sodium bicarbonate, sodium carbonate, sodium chloride, sodium hydroxide, sodium perchlorate (monohydrate), and Triton X-100 were purchased from Thermo Fisher Scientific. Anhydrous methanol, conc. hydrochloric acid, and hydrogen peroxide (30 % v/v) were purchased from Macron Fine Chemicals. Zinc dust was purchased from Mallinckrodt Incorporated. Acetic anhydride, adenosine triphosphate, anhydrous acetonitrile, anhydrous dichloromethane, anhydrous dimethylformamide, arachidic acid, arachidonic acid, β-Nicotinamide adenine dinucleotide 2′-phosphate reduced tetrasodium salt hydrate (NADPH), calcium chloride, catalase from bovine liver (lyophilized), celite 545, copper(II) chloride, esterase from porcine liver (lyophilized), formaldehyde (37 % w/w in water), glutathione (reduced), glyoxal (40 % w/w in water), hemin from bovine, hexanes, horseradish peroxidase (type 1), L-ascorbic acid, L-cysteine, L-dehydroascorbic acid, lipopolysaccharides from Escherichia coli O111:B4 (purified by phenol extraction), manganese(II) chloride, myeloperoxidase from human leukocytes, *p*-nitrophenylacetate, potassium superoxide, propidium iodide, rat liver microsomes (pooled, male), resazurin, sodium acetate, sodium hydrosulfide (hydrate), sodium metal, tris base, and trypan blue powder were purchased from Millipore-Sigma Aldrich. Porcine hematin was purchased from MP Biomedical LLC. 4-dimethylaminopyridine, potassium iodide and sodium sulfate (anhydrous) were purchased from Oakwood Chemicals. *N*-ethylmaleimide was purchased from Pierce Chemical Company. Celecoxib, indomethacin, phenol, and resorufin were purchased from Tokyo Chemical Industry. L-buthionine-(S,R)-sulfoximine was purchased from Toronto Research Chemicals.

Instruments and Software. ^{1}H and ^{13}C NMR spectra were acquired on the Varian 500 or Carver B500 spectrometer. The following abbreviations were used to describe coupling constants: singlet (s), doublet (d), triplet (t), or multiplet (m). Spectra were visualized and analyzed using MestReNova (version 10.0) and referenced to trace non-deuterated solvent. High-resolution mass spectra were acquired on a Waters Q-TOF Ultima ESI mass spectrometer or a Waters Synapt G2-Si ESI/LC-MS spectrometer. Ultraviolet-visible spectroscopy was performed on a Cary 60 or NanoDrop 2000 spectrometer. Fluorescence spectra were acquired on a QuantaMaster-400 scanning spectrofluorometer or SpectraMax M2 plate reader. Ultraviolet-visible spectroscopy and fluorimetry was performed with a micro fluorescence quartz cuvette (Science Outlet), sub-mircroquartz fluorimeter cell (Starna Cells, Inc.), or 96-well plates (clear or black with flat bottom, Corning). Refractive indices were measured using a RHB-32ATC Brix Refractometer. A Strathkelvin oxygen electrode was used for measuring cyclooxygenase activity. Cells were visualized on an EVOS FL epifluorescence microscope and

cellular imaging was performed using a Zeiss LSM 700 confocal microscope. Countess® II FL Automated Cell Counter was used for cell viability assays. Flow cytometry was performed on a BD LSR Fortessa Flow Cytometry Analyzer. Confocal images and flow data were analyzed using ImageJ (NIH)[1] and FCS Express 6.04, respectively. Data were analyzed using Microsoft Excel and GraphPad Prism (version 6.0 or 8.0) and final figures were prepared in Adobe Illustrator (version 22.0.2).

Synthetic Procedures. Thin-layer chromatography (TLC) was performed on glass-backed TLC plates precoated with silica gel containing an UV254 fluorescent indicator (Macherey-Nagel). TLC's were visualized with a 254/365 nm UV hand-held lamp (UVP). Flash silica gel chromatography was performed using 0.04 – 0.063 mm 60 M silica (Macherey-Nagel). All glassware used under anhydrous reaction conditions were flame-dried under vacuum and cooled immediately before use.

10H-phenoxazine-3,7-diyl diacetate (1). The compound was prepared according to the previous report by Kodera and coworkers.[2] Briefly, a mixture of resazurin (200. mg, 0.796 mmol, 1 equiv) and zinc dust (240. mg, 3.67 mmol, 4.6 equiv) in glacial acetic acid (6 mL) was stirred at room temperature for 2 h under N_2 atmosphere in the dark. The reaction was concentrated under inert atmosphere, dissolved in acetone (4 mL) and treated with DMAP (68.4 mg, 0.560 mmol, 0.7 equiv) and then acetic anhydride (0.16 mL, 1.693 mmol, 2.1 equiv) was added dropwise and stirred under N_2 atmosphere in dark for 3 h. After completion, the reaction was concentrated and then purified via silica gel chromatography (eluent: 20% EtOAc in hexanes) to afford the product as a yellow solid (150. mg, 0.501 mmol, 63% yield). ^{1}H NMR (500 MHz, $CDCl_3$) δ 6.45 (dd, *J* = 8.4, 2.2 Hz, 2H), 6.39 (d, *J* = 2.0 Hz, 2H), 6.26 (d, *J* = 8.4 Hz, 2H), 5.32 (s, 1H), 2.25 (s, 6H). 13C NMR (125 MHz, $CDCl_3$) δ 169.76, 144.59, 142.94, 129.24, 116.25, 113.12, 109.88, 21.02. HRMS $[M+H]^+$ calculated mass for $C_{16}H_{14}NO_5$ = 300.0872, found = 300.0879.

10-((5Z,8Z,11Z,14Z)-icosa-5,8,11,14-tetraenoyl)-10H-phenoxazine-3,7-diyl diacetate (2). A solution of **1** (61.2 mg, 0.204 mmol, 1.1 equiv) in anhydrous acetonitrile (1.2 mL) was treated sequentially with Na_2CO_3 (23.6 mg, 0.223 mmol, 1.2 equiv) and then arachidonoyl chloride[3] (60.0 mg, 0.186 mmol, 1 equiv) in dry acetonitrile (1 mL) at 0 ºC. The reaction was allowed to warm to room temperature before potassium iodide (83.3 mg, 0.502 mmol, 2.7 equiv) was added and the mixture was allowed to continue for 5 h under N_2 atmosphere in the dark. Once complete, the reaction was filtered, washed with EtOAc (3×), concentrated and purified by silica gel chromatography (eluent: 90% CH_2Cl_2 in hexanes) to obtain the product as an orange solid (53.3 mg, 0.091 mmol, 49% yield). ^{1}H NMR (500 MHz, $CDCl_3$) δ 7.44 (d, *J* = 8.7 Hz, 2H), 6.95 – 6.85 (m, 4H), 5.45 – 5.25 (m, 8H), 2.84 – 2.73 (m, 6H), 2.59 (t, *J* = 7.4 Hz, 2H), 2.30 (s, 6H), 2.07 (dq, *J* = 21.7, 7.3 Hz, 4H), 1.75 (q, *J* = 7.4 Hz, 2H), 1.39 – 1.26 (m, 6H), 0.88 (t, *J* = 6.8 Hz, 3H). ^{13}C NMR (125 MHz, $CDCl_3$) δ 171.84, 168.98, 151.18, 148.79, 130.42, 128.93, 128.85, 128.49, 128.12, 128.09, 127.82, 127.49, 126.74, 125.42, 116.62, 110.80, 33.39, 31.46, 29.27, 27.16, 26.42, 25.58, 25.57, 25.53, 24.90, 22.52, 21.02, 14.03. HRMS $[M+H]^+$ calculated mass for $C_{36}H_{44}NO_6$ = 586.3169, found = 586.3180.

CoxFluor. A solution of **2** (50. mg, 0.085 mmol, 1 equiv) in anhydrous MeOH (3 mL) was treated with Na (2 mg, 0.087 mmol, 1 equiv) at 0 ºC and the reaction was allowed to continue at the same temperature for 0.5 h. When complete, the reaction was treated with aq. satd. $NaHCO_3$ and extracted with EtOAc (3×). The organic layer was dried over anhydrous sodium sulfate and purified by silica gel chromatography (eluent: 1% MeOH in CH_2Cl_2) to afford the product as an off-white solid (29.2 mg, 58.2 μmol, 68% yield). ^{1}H NMR (500 MHz, CD_3OD) δ 7.88 (s, 2H), 7.28 (d, *J* = 8.8 Hz, 2H), 6.59 – 6.55 (m, 4H), 5.39 – 5.24 (m, 8H), 2.80 (q, *J* = 5.4 Hz, 4H), 2.74 (t, *J* = 6.7 Hz, 2H), 2.60 (t, *J* = 7.3 Hz, 2H), 2.04 (dt, *J* = 11.7, 5.8 Hz, 4H), 1.66 (q, *J* = 7.3 Hz, 2H), 1.38 – 1.29 (m, 6H), 0.88 (t, *J* = 7.0 Hz, 3H). ^{13}C NMR (125 MHz, $CDCl_3$) δ 173.29, 154.95, 151.90, 130.52, 128.96, 128.84, 128.55, 128.15, 127.87, 127.52, 125.64, 121.95, 110.44, 104.29, 33.36, 31.49, 29.69, 29.30, 27.20, 26.51, 25.62, 25.59, 25.55, 25.02, 22.56, 14.07. HRMS $[M+H]^+$ calculated mass for $C_{32}H_{40}NO_4$ = 502.2957, found = 502.2943.

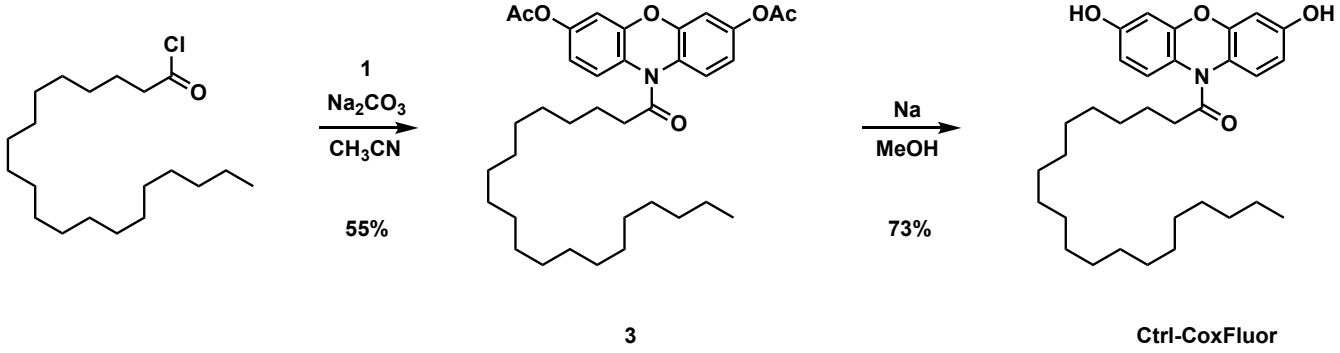

Scheme S1. Synthesis **Ctrl-CoxFluor**.

Arachidoyl Chloride. The material was prepared in an identical manner to arachidonoyl chloride according to a previously reported protocol.[3] Briefly, arachidic acid (50 mg, 0.160 mmol, 1.0 equiv) was dissolved in anhydrous CH_2Cl_2 (1 mL) and anhydrous DMF (30 μL) and placed under N_2 atmosphere. The solution was cooled to -5 ºC in an ammonium chloride ice bath before oxalyl chloride (28 μL, 0.326 mmol, 2.0 equiv) in anhydrous CH_2Cl_2 (200 μL) was added. The reaction was maintained at the same temperature for 4 h and then allowed to sit at -20 ºC overnight. The reaction was complete according to crude NMR and then it was concentrated. The residue was purified by dissolving in hexanes, filtering, and re-concentrating the filtrate. The material was used without purification.

10-icosanoyl-10H-phenoxazine-3,7-diyl diacetate (3). 1 (49.7 mg, 0.166 mmol, 1.1 equiv) in anhydrous acetonitrile (3 mL) was cooled to 0 ºC and treated with Na_2CO_3 (19.2 mg, 0.181 mmol, 1.2 eq). A solution of arachidoyl chloride (50 mg, 0.151 mmol, 1 equiv) in anhydrous acetonitrile (3 mL) was added dropwise and allowed to warm to room temperature. Next, potassium iodide (124 mg, 0.747 mmol, 4.9 eq) was added and the mixture was allowed to stir at room temperature for 5 h under N_2 atmosphere in the dark. Once complete, the reaction was filtered, washed with EtOAc (3×), concentrated and purified by silica gel chromatography (eluent: 90% CH_2Cl_2 in hexanes) to obtain the product as a white solid (50.0 mg, 84.2 μmol, 55% yield). ^{1}H NMR (500 MHz, $CDCl_3$) δ 7.45 (d, J = 8.6 Hz, 2H), 6.94 – 6.85 (m, 4H), 2.57 (t, J = 7.5 Hz, 2H), 2.30 (s, 6H), 1.64 (q, J = 7.3 Hz, 2H), 1.24 (m, 32H), 0.88 (t, J = 6.8 Hz, 3H). ^{13}C NMR (125 MHz, $CDCl_3$) δ 172.20, 169.05, 151.24, 148.78, 126.87, 125.45, 116.65, 110.81, 34.06, 31.91, 29.69, 29.66, 29.63, 29.57, 29.42, 29.38, 29.35, 29.15, 25.30, 22.68, 21.06, 14.12. HRMS $[M + H]^+$ calculated mass for $C_{36}H_{52}NO_6$ = 594.3795, found = 594.3806.

Ctrl-CoxFluor. To a suspension of compound **3** (40. mg, 0.067 mmol, 1eq) in dry MeOH (3 mL) at 0 ºC was added Na (2 mg, 0.087 mmol, 1.3 equiv) and the reaction was stirred for 0.5 h. After completion, the reaction was treated with aq. satd. $NaHCO_3$ and extracted with EtOAc (3×). The organic layer concentrated and purified by silica gel chromatography (eluent: 1% MeOH in CH_2Cl_2) to afford the product as a white solid (25 mg, 49 μmol, 73% yield). ^{1}H NMR (500 MHz, $CDCl_3$) δ 7.17 (d, *J* = 7.5 Hz, 2H), 6.58 – 6.43 (m, 4H), 2.47 (t, *J* = 7.5 Hz, 2H), 1.53 (q, *J* = 7.2, 6.7 Hz, 2H), 1.17 (d, *J* = 13.3 Hz, 32H), 0.81 (t, *J* = 6.9 Hz, 3H). ^{13}C NMR (125 MHz, $(CD_3)_2CO$) δ 172.85, 157.04, 152.83, 126.86, 122.80, 110.85, 104.21, 34.34, 32.65, 30.40, 30.37, 30.22, 30.09, 29.84, 25.96, 23.34, 14.36. HRMS $[M+H]^+$ calculated mass for $C_{32}H_{48}NO_4$ = 510.3583, found = 510.3583.

Photophysical Characterization. Extinction coefficients and fluorescence quantum yields were acquired (*n* = 3) and reported as the average with a standard deviation less than 15%. Extinction coefficients were acquired by titrating compound in 100 mM Tris-HCl (pH 8.0) within the linear range. Fluorescence quantum yields were obtained using the modified method for relative fluorescence quantum yield.[4] Dye was titrated into solution and the absorbance and emission was monitored with excitation at 540 nm. The absorbance was maintained below 0.1 to limit secondary absorbance events. Total emission spectra were integrated, and the relative quantum yield was calculated relative to Rhodamine B (ϕ = 0.70, ethanol).[5] The refractive index of 100 mM Tris-HCl (pH 8.0) was measured to be 1.33514.

SUPPORTING INFORMATION

Protein Expression and Purification. Human COX-2-His_6 was expressed[6,7] and purified according to previously reported protocols.[8] The purification of COX-1 was carried out based on a previous protocols with minor modifications.[9,10] Bovine seminal vesicles (~25 g) were obtained from a butcher (Arends Farms Meats and Butcher Shop, Ivesdale, IL) and were mechanically homogenized using a Bio-homogenizer 2-speed (Model no. M133/1281-0) in 50 ml buffer A (50 mM Tris-HCl, 5 mM EDTA, 5 mM DETC, 1 mM phenol, pH 8.0). Note that all centrifugation was performed at 4 °C on a Sorvall RC 6+ centrifuge with a Fiberlite F21 8x50 y rotor for less than 10,000 rpm and Sorvall WX Ultra 80 with a SureSpin 630 rotor equipped with a swinging bucket for more than 10,000 rpm. Once homogenized, cellular debris was removed via centrifugation at 9,500 rpm for 15 minutes. The supernatant was collected and centrifuged at 30,000 rpm for 1 h to obtain the microsomal pellet containing COX-1. This pellet was resuspended in 50 ml buffer B (50 mM Tris-HCl, 1 mM EDTA, 0.1 mM $NaClO_4$, 0.1 mM DETC, 0.5 mM phenol, pH 8.0), using a homogenizer, before centrifugation at 30,000 rpm for 1 h. The corresponding pellet was resuspended in 50 ml buffer C (50 mM Tris-HCl, 1 mM EDTA, 1 mM phenol, pH 8.0), 10% Triton X-100 was added dropwise with stirring until a final concentration of 1% (v/v) was obtained, and the resulting solution was allowed to stir for 1 h at 4 °C. A final centrifugation at 30,000 rpm was performed for 1 h before the supernatant was loaded onto a DEAE-Sepharose column (GoldBio) that was previously equilibrated with buffer C. The column was washed with 40 mL buffer C and then COX-1 was eluted using a stepwise NaCl gradient prepared from different ratios of buffer C to buffer D (50 mM Tris-HCl, 1 mM EDTA, 1 mM phenol, 400 mM NaCl, pH 8.0). Specifically, the column was washed with sequential 40 mL portions at each concentration (90% buffer C – 0% buffer C in 10% steps). A Bradford assay (Thermo Scientific) was used to determine which fractions contained eluted protein; these fractions were concentrated and frozen after the addition of glycerol (10% v/v final). Porcine hematin (1 mM) was titrated into concentrated protein until λ_{407} stabilized at a maximum. Human CYP2J2 cDNA was obtained from OriGene (Catalog No. SC321730) and N-terminally modified.[11] This truncated M2D34G-CYP2J2 was expressed and purified via Ni-NTA chromatography (GoldBio) as previously published.[11–13] Full length R. norvegicus cytochrome P450 reductase (CPR) was expressed and purified via ADP-agarose chromatography (GoldBio) following previously published protocols.[14] Protein concentration for COX-1 and COX-2 (MW = 140 kDa). were determined using the bicinchoninic acid assay (BCA Assay, Thermo Fisher Scientific) relative to a bovine serum albumin standard according to the manufacturer's protocol and the molecular weights for all proteins were calculated using the ExPASy tool.[15] CYP2J2 (MW = 57 kDa, ε = 110 $mM^{-1}cm^{-1}$ λ_{max} = 417 nm) and CPR (MW = 77 kDa, ε = 21.4 $mM^{-1}cm^{-1}$ λ_{max} = 454 nm) were quantified spectroscopically using their Soret absorbance.

Fluorimeter Fluorescence Assay. The fluorescence assays were performed in microquartz cuvettes or submicroquartz cuvettes with a maximum volume of 600 μL. Reactions were monitored at room temperature using 540 nm excitation and emission was collected from 550-700 nm with a slit width of 1.25 mm. Total volumes of the reaction mixtures were maintained at 570 μL. To 100 mM Tris-HCl buffer (480 μL, pH 8.0) was added hemin (30 μL, 19 μM in 4% DMSO in 100 mM Tris-HCl, pH 8.0), COX-2 (30 μL, 4.75 μM 100 mM Tris-HCl, pH 8.0) and the reaction was initiated with CoxFluor (30 μL, 190 μM 10% DMSO in 100 mM Tris-HCl, pH 8.0). Final reaction concentrations were 1 μM hemin, 250 nM COX-2 and 10 μM CoxFluor in 100 mM Tris-HCl with 1.26% DMSO (v/v). Experiments in the presence of reduced GSH were conducted according to the same procedure, but GSH (30 μL, 19 mM in 100 mM Tris-HCl, pH 8.0) was added before the addition of CoxFluor for a final concentration of 1 mM. Assays performed in submicroquartz cuvettes were performed maintaining the same ratios, but with a final volume of 142.5 μL.

Plate reader Fluorescence Assay. The fluorescence assays were performed at room temperature using 540 nm excitation and 590 nm emission. Total volume of the reaction mixture was maintained at 190 μL. To 100 mM Tris-HCl buffer (160 μL, pH 8.0) was added hemin (10 μL, 3.8 μM in 4% DMSO in 100 mM Tris-HCl, pH 8.0), COX-2 (10 μL, 950 nM in 100 mM Tris-HCl buffer, pH 8.0) and the reaction was initiated with CoxFluor (10 μL, 190 μM in 10% DMSO in 100 mM Tris-HCl, pH 8.0). Final reaction concentrations were 200 nM hemin, 50 nM COX-2 and 10 μM CoxFluor in 100 mM Tris-HCl with 1.26% DMSO (v/v). Inhibition assays were performed according to the same procedure, but COX-2 was preincubated with hemin and inhibitor for 0.5 h at 0 °C before initiation with CoxFluor. Relative fluorescence enhancement is calculated by comparing to a buffer control with 10 μM CoxFluor.

Enzyme Selectivity. Enzyme activity was defined as the amount substrate (μmol) consumed during one minute by one milligram of enzyme in 100 mM Tris-HCl at pH 8.0 under saturating conditions. Enzyme concentrations were measured using the BCA assay

(Thermo Fisher Scientific) according to the published protocol with bovine serum albumin for the standard curve. COX-1 and COX-2 cyclooxygenase activities were measured using Strathkelvin oxygen electrode with arachidonic acid (200 μM). The oxygen electrode was calibrated using 1% sodium sulfite for 0% oxygen and atmosphere equilibrated 100 mM Tris-HCl at pH 8.0 for 100% oxygen. The reaction was monitored at 37 ºC in a glass chamber with total reaction volume of 1 mL. Hemin (5 μM), phenol (1 mM), and COX (2 μg) were added to atmosphere equilibrated buffer and then the reaction was initiated with AA (200 μM). Porcine esterase activity was measured spectroscopically at 405 nm using *p*-nitrophenyl acetate (1.5 mM) as the substrate. Bovine catalase activity was measured using a discontinuous Amplex® Red-horseradish peroxidase assay to confirm the amount of hydrogen peroxide (initially 31.25 μM) remaining after 0.5 h incubation with excitation at 540 nm and emission at 590 nm. CYP2J2 activity was measured spectroscopically at 340 nm using cytochrome P reductase (3-fold excess), NADPH (1 mM), and arachidonic acid (70 μM) as the substrate. Rat liver microsomes were performed at concentrations ranging from 12.5 μg/mL to 200 μg/mL and the largest turn-on was reported. Horseradish peroxidase activity was measured using hydrogen peroxide (31.25 μM) and Amplex® Red (50 μM) as the substrates with excitation at 540 nm and emission at 590 nm. Myeloperoxidase selectivity was measured using the manufacturer's conditions (50 mM sodium acetate, pH 6.0, 100 mM NaCl) because the lysosomal enzyme is inactive at pH 8.0. Selectivity was assessed using 10-fold excess protein and the solution was brought to a pH of 8.0 after 4 h with 0.5 M aq. NaOH prior to measurement. Monoamine oxidase A selectivity was assessed using human supersomes with 10-fold excess protein (350 μg/mL) under the standard COX conditions. 5-lipoxygenase selectivity was performed using the manufacturer's protocol and reported activity. Specifically, the active recombinant human protein in the insect cell lysate was diluted for a final activity of 1.01 U in 50 mM Tris-HCl buffer (pH 7.5) containing 2 mM $CaCl_2$, 1 mM ATP, and 4.6 μM 13(S)-HpODE. Prior to measuring the fluorescence, the solution was titrated with 0.5 M aq. NaOH for a pH 8.0. When measured, all enzyme activities were confirmed to be under saturating conditions and within the first 20% of the reaction. The selectivity of CoxFluor (10 μM) was monitored after incubation with either 0.101 U COX-2 or 1.01 U of the other enzymes, unless noted otherwise above, in 100 mM Tris-HCl buffer at pH 8.0 using the plate reader with excitation at 540 nm and emission at 590 nm. Total reaction volume was maintained at 95 μL with a final DMSO concentration of 1.26% (v/v). Relative fluorescence enhancement is calculated by comparing to a buffer control containing 10 μM CoxFluor.

Analyte Selectivity. Response of CoxFluor (10 μM) to a variety of reactive oxygen, nitrogen, carbonyl, metals and sulfur species (50 equiv) were monitored using the plate reader assay. Total volume of the reaction mixture was maintained at 190 μL in 100 mM Tris-HCl buffer (pH 8.0) with a final DMSO concentration of 1.26% (v/v). Assays for CoxFluor or resorufin were initiated by the addition of the analytes and the reactions were incubated at room temperature for 4 h. Measurements were recorded at a range of time points, and the relative turn-on was determined relative to a buffer control containing 10 μM CoxFluor or resorufin. Superoxide anion was added as a solution of potassium superoxide in DMSO. Nitroxyl was generated in situ from a solution of Angeli's salt in degassed 10 mM potassium hydroxide solution. Angeli's salt was prepared according to previously reported literature.[16] NO was generated in situ from a solution of MAHMA-NONOate in degassed 10 mM potassium hydroxide. Peroxynitrite was prepared according to previously reported literature.[17] All metals were prepared from their chloride salt. Formaldehyde solutions were prepared by depolymerizing saturated aqueous solutions at 100 ºC before use. Dehydroascorbic acid was prepared by dissolving the solid at 65 ºC in water before cooling to room temperature for use. All other analytes were prepared by dilution or dissolution from commercially available sources. All metal solutions were prepared from their chloride salts.

Structure Preparation for Molecular Dynamics Simulations and Ensemble Molecular Docking. The preferential binding of CoxFluor to COX-2 over COX-1 was probed using ensemble docking and molecular dynamics techniques. The structure of sheep COX-1 (PDB 5U6X)[18] and human COX-2 (PDB 5KIR)[19] were obtained from X-ray diffraction data. Before simulations, all non-heme cofactors were removed; the heme bound cobalt in COX-2 was replaced with an iron; cysteine bridges and the iron histidine were patched and preserved using PSFGEN; and the coordinates and topology for missing hydrogens were predicted using PSFGEN. To validate the selected structures, we calculated root mean squared deviation (RMSD) for 5U6X and 5KIR versus a myriad of resolved structures using SuperPose (Tables S1-2).[20]

SUPPORTING INFORMATION

Equilibrium Molecular Dynamics Simulations of COX-1 and COX-2. Parameters and protocols for simulations were followed according to literature precedence with minor modifications.[21,22] Molecular dynamics simulations were performed using NAMD 2.12[23] with the CHARMM36m force field.[24] Constant temperature and pressure were maintained using Langevin dynamics and Langevin piston Nosé−Hoover methods[25,26] at 310 K and 1 atmosphere, respectively. The particle mesh Ewald (PME) method was used to calculate long-range electrostatic forces[27,28] using a 1 Å grid spacing. The van der Waals interactions were evaluated with a cutoff of 12 Å, with a force-based switching scheme after 10 Å. A 2 fs integration time step was applied with the SETTLE algorithm.[29] VMD 1.9.3 was used for visualization and analysis.[30] Both COX-1 and COX-2 were first equilibrated for 10 ns with the entire protein restrained (1.0 kcal/mol/Å^2) to allow for solvation of the protein, followed by progressively decreasing harmonic restraints over the course of 10 ns on protein Cα atoms (2.5 ns at 1.0 kcal/mol/Å^2, 2.5 ns at 0.75 kcal/mol/Å^2, 2.5 ns at 0.50 kcal/mol/Å^2, 2.5 ns at 0.25 kcal/mol/Å^2). This was followed by 200 ns production simulation without restraints. RMSD was calculated using MDAnalysis[31,32] for the simulation trajectories AA bound crystal structures of COX-1 (PDB 1DIY)[33] and COX-2 (PDB 3HS5)[6] to confirm no major deviations.

Ensemble Molecular Docking. Ensemble docking of CoxFluor to COX-1 and COX-2 was performed using AutoDock Vina.[34] The previously discussed simulations were used to sample the dynamics of COX-1 and COX-2 for docking. Because both COX-1 and COX-2 are homodimers in the crystallographic state it was possible to double the sampling time by overlaying the monomers throughout the docking process for a total of 400 ns sampling time (200 ns sampling time for docking to each monomer). For each snapshot, a 26 × 26 × 26 Å^3 cube containing both the cyclooxygenase and peroxidase active sites was used to fully sample the suspected binding sites. Each snapshot was docked with an exhaustiveness of 10, yielding a maximum of 4000 docked poses. These poses where then characterized based on location and binding affinities. To determine the location of the binding, poses were grouped based off of their proximity to the iron, within the heme, where greater than 8 Å was defined as cyclooxygenase binding (confirmed that this cutoff was consistent with structural understanding of the protein). The same protocol for docking was implemented for the CoxFluor-PGG_2 intermediate. Docking within the cyclooxygenase site was performed within a 22 × 22 × 22 Å^3 cube using the same protocol where the box only included the cyclooxygenase active site. Using the VMD plugin Multiseq,[35] a STAMP structural alignment was done on 5U6X and 1DIY, as well as on 5KIR and 3HS5 to identify relevant AA positions in COX-1 and COX-2 respectively, followed by visualization in PYMOL (Version 1.7.0.0; Schrodinger, LLC).

CoxFluor, Ctrl-CoxFluor & Resorufin Stability Assays. Stability assays were performed in a plate reader in triplicate with 10 μM of each compound in buffers/solvent (100 mM Tris-HCl at pH 8, DMEM with 10% FBS, DMEM without serum and DMSO) at room temperature or 37 ºC in the absence or presence of ambient light for 8 h. Fluorescence was measured using the plate reader with excitation at 540 nm and emission from 560-700 nm and the relative turn-on was determined by the change of fluorescence intensity at 590 nm.

Cell Culture. HEK 293T and RAW 264.7 macrophage cells were acquired from ATCC and Prof. Elvira de Mejia (Food Science and Human Nutrition, UIUC), respectively. Cells were cultured in phenol-red free Dulbecco's modified eagle medium (DMEM, Corning) supplemented with 10% fetal bovine serum (FBS, Sigma Aldrich), and 1% penicillin/streptomycin (Corning). Incubation with 0.25% trypsin containing EDTA and phenol red (Gibco^{TM}, Fisher Scientific) or manual scrapping is used for passaging for HEK 293T and RAW 264.7 macrophage cells, respectively. Cells were incubated at 37 °C with 5% CO_2. Experiments were performed in 4-well chambered cover glasses (Lab-Tek, Thermo Scientific) or 6-well plates (BioLite, Thermo Scientific).

Trypan Blue Exclusion Cytotoxicity Assay. 6-well plates were seeded with 300,000 cells per well (2 mL of 150,000 cells/mL) and incubated at 37 °C with 5% CO_2 for 48-72 h (~60-80% confluent). Media was removed and replaced with either 5, 10, or 25 μM CoxFluor in fresh serum-free DMEM media (1.25% DMSO v/v final concentration). After 6 h the media was removed, and cells were trypsinized with 200 μL 0.25% trypsin-EDTA for less than 5 minutes at 37 °C. The trypsin was quenched with the addition of 1.8 mL DMEM media containing 10% FBS and the cells were mixed thoroughly before diluting 1:1 with trypan blue (0.4% in PBS w/v). Percent viability was measured using Countess® II FL Automated Cell Counter (Thermo Fisher Scientific) where the parameters were optimized to identify live and dead cells. Viability was calculated by the relative to the vehicle control.

MTT Cytotoxicity Assay. 96-well plate was seeded with 20,000 cells per well (200 μL of 100,000 cells/mL, RAW 264.7 macrophage) or 25,000 cells per well (200 μL of 125,000 cells/mL, HEK 293T cells) and incubated at 37 °C with 5% CO_2 for 72 h (~90% confluent). Media was removed and fresh serum-free DMEM media containing 0, 5, 10, or 25 μM CoxFluor (1.25% DMSO final v/v) was added. The media was removed at various time points (3 or 6 h) and replaced with 200 μL 20:1 mixture of FBS-free DMEM and (3- (4,5-dimethylthiazol-2-yl)-2,5-diphenyl-tetrazolium bromide (MTT, 5 mg/mL stock in PBS). The cells were incubated for 4 h under the same conditions and then the medium was removed and replaced with DMSO (200 μL/well). The absorbance of each well was recorded after a 1:5 dilution in DMSO at 555 nm on a microplate reader. Viability was calculated by the absorbance relative to the vehicle control.

HEK293T Transfection with human COX-2. The plasmid containing human COX-2 (pcDNA3.1-hPTGS2-2flag) was purchased from Addgene (Catalog# 102498, deposited by Prof. Jun Yu, The Chinese University of Hong Kong).[36] The plasmid was isolated from a single colony that was grown to turbidity overnight at 37 °C in Luria broth (LB) media with 100 μg/mL ampicillin (5 mL) using the GeneJET plasmid Miniprep (Thermo Scientific) according to the manufacturer's protocol, however the plasmid was eluted with Milli-Q water rather than the elution buffer. Plasmid concentration was determined using the absorbance at 260 nm on a NanoDrop 2000 instrument (Thermo Scientific). Prior to plating onto 4-well chambered cover glasses (Lab-Tek, Thermo Scientific) the surface exposed substrate was coated with R&D Systems™ Cultrex Poly-L-Lysine (Fisher Scientific) according to the manufacturers protocol (allowed to dry > 3 h). Plates were seeded with 175,000 cells per well (500 μL of 350,000 cells/mL in DMEM media supplemented with 10% FBS) and allowed the cells to incubate for 40 h at 37 °C with 5% CO_2 (60-70% confluent). Transfections was performed using Lipofectamine 3000 (Thermo Fisher Scientific) according to the manufacturer's protocol. Briefly, 180 μL of transfection master mix was prepared by a 1:1 dilution of lipofectamine 3000 reagent (5.4 μL in 90 μL Opti-MEM™ Reduced Serum Media) and DNA complexed to P3000 reagent (1,800 ng plasmid with 3.6 μL P3000 in Opti-MEM™ Reduced Serum Media) and the master mix was allowed to incubate at room temperature for 5 to 10 minutes. Media was removed from each well and replaced with 500 μL Opti-MEM™ Reduced Serum Media followed by the addition of 20 μL transfection master mix. After 48 h incubation at 37 °C with 5% CO_2 (~90-100% confluent) the cells were subjected to experimental conditions for imaging.

Confocal Fluorescence Live-Cell Imaging of human COX-2 Transfected HEK 293T cells. Transfections were performed using the Lipofectamine 3000 reagent according to the aforementioned protocol. Control wells were treated the same as the transfected wells without the addition off the transfection master mix. The media was removed from each well and replaced with serum-free DMEM media containing 10 μM CoxFluor or 10 μM CoxFluor with 10 μM indomethacin (1 % DMSO final concentration). Cells were incubated at 37 °C with 5 % CO_2 for 3 h and then imaged using 555 nm excitation with emission collected from 565-700 nm. Each well was imaged using a Zeiss LSM 700 confocal microscope (n = 3 technical replicates; n = 4 biological replicates). For GSH knockdown experiments, the initial media change was performed with 1 mM NEM (0.1 % DMSO final concentration) in serum-free DMEM media and the cells were allowed to incubate for 30 minutes before proceeding to the staining with CoxFluor. Images were quantified over the entire imaging window, without any processing, using ImageJ (v. 1.51, NIH). All publication images were processed using identical parameters and false colored (LUT: jet.lut) in ImageJ.[1]

RAW 264.7 Macrophage Activity Assays. 6-well plates (BioLite, Thermo Scientific) were seeded with 250,000 cells per well (2.0 mL of 120,000 cells/mL) and the cells were allowed to incubate at 37 °C with 5 % CO_2 for 72 h (~70-80% confluent). The media was removed and replaced with serum-free DMEM (1.98 mL). Lipopolysaccharide was added in PBS (20 μL 100 μg/mL for final concentration of 1 μg/mL) at 2, 4, 6, 8, 10, 19, and 24 h (n = 3 biological replicates). Control wells were prepared by adding PBS without LPS at the 24 h time point. The media was removed, and the cells were lysed by adding CelLytic M (200 μL, Millipore-Sigma) and mixing for 15 minutes at room temperature. The solution was mixed well via pipette followed by vortex for 10 seconds. Cellular debris was removed by centrifugation using a Fisher Scientific accuSpin Micro 17R centrifuge at 6,000 rpm for 10 minutes (4 °C). The samples were stored at 4 °C and activity was measured immediately. Activity was measured according to a modified fluorimeter assay with excitation at 540 nm, emission at 590 nm, and slit width of 0.8 mm. Specifically, to a solution of 888 μL 100 mM Tris-HCl buffer (pH 8.0) and 100 μL lysate was added 10 μL 100 mM *N*-ethylmaleimide (1 mM final concentration) and the solution was allowed to incubate at room temperature for 1 minute. The reaction was initiated with 2 μL 2 mM CoxFluor (4 μM final concentration, 1.2% DMSO final) and

the kinetics were monitored over 2 minutes. Rates were measured within the linear region (usually the first 30 seconds after initiating the reaction). A calibration curve was constructed with resorufin in buffer containing 1 mM *N*-ethylmaleimide, 10% CelLytic M, and a final DMSO concentration of 1.2%. Total protein concentration was measured using the BCA assay (Thermo Fisher Scientific) to calculate COX-2's specific activity.

Confocal Fluorescence Live-Cell Imaging of Lipopolysaccharide-activated RAW 264.7 Macrophages. The surface exposed substrate of 4-well chambered cover glasses (Lab-Tek, Thermo Scientific) were coated with R&D Systems™ Cultrex Poly-L-Lysine (Fisher Scientific) according to the manufacturers protocol. Plates were seeded with 180,000 RAW 264.7 macrophage cells per well (500 µL of 360,000 cells/mL in DMEM media supplemented with 10% FBS) and allowed the cells to incubate for 38 h at 37 °C with 5 % CO_2 (70-80% confluent). The media was removed and replaced with serum-free DMEM containing either PBS or 1 µg/mL lipopolysaccharide in PBS and 0.2 mM BSO (500 µL final volume). The cells were incubated under these conditions for 17 h at 37 °C with 5% CO_2. Next, the media was removed and replaced with the same conditions either with or without indomethacin (10 µM) and the cells were allowed to incubate for 2 h at 37 °C with 5% CO_2 (500 µL final volume containing 0.2% DMSO final concentration). The media was removed the cells were stained under identical conditions in addition to 10 µM CoxFluor (500 µL final volume containing 1.5% DMSO final concentration). After incubation at 37 °C with 5 % CO_2 for 4 h, each well was imaged using a Zeiss LSM 700 confocal microscope (n = 3 technical replicates; n = 4 biological replicates). Images were quantified over the entire imaging window, without any processing, using ImageJ (v. 1.51, NIH). All publication images were processed using identical parameters and false colored (LUT: jet.lut) in ImageJ.[1]

Flow Cytometry of Lipopolysaccharide-induced COX-2 Expression in RAW 264.7 Macrophages. RAW 264.7 macrophage cells (300,000 cells, 2 mL of 150,000 cells/mL) were seeded into 6-well plates and incubated for 48 to 72 h under standard conditions for a final confluency of ~60-80%. The media was removed and replaced with serum-free DMEM (1.98 mL) followed by LPS (1 µg/mL final concentration, 20 µL of 100 µg/mL in PBS) at 4 or 19 h before collection. Cellular GSH was depleted 2 h prior to collection via treatment with BSO (0.2 mM final concentration, 40 µL 10 mM solution in 1:1 DMSO: serum-free DMEM, 1% DMSO final concentration). Cells were collected by treatment with 0.5 mL 0.25% trypsin-EDTA for less than 5 minutes at 37 ºC and then the trypsin was inactivated with 1.0 mL DMEM media containing 10% FBS. The solution was partitioned for two samples, which were subsequently collected via centrifugation at 6,000 RPM at 4 ºC in 1.6 mL Eppendorf tubes. The media was removed, and cells were resuspended in 0.2 mM BSO with or without 10 µM CoxFluor (1 mL, 1.5% DMSO final concentration in serum-free DMEM) for 90 minutes at 37 ºC with agitation. When performing inhibition studies, the aforementioned staining solutions were prepared with 20 µM indomethacin without affecting the final concentration of DMSO. After staining, cells were pelleted using the aforementioned procedure and were resuspended in PBS. Samples were stored on ice prior to analysis on a BD LSR Fortessa Flow Cytometry Analyzer with 561 nm excitation and 582/15 emission bandpass filter. Dead cells were excluded from the analysis by staining samples (~300 µL) with propidium iodide (1 µL of 1 mg/mL in deionized water) for 5-10 minutes at room temperature before analysis with 561 nm excitation and 595 nm longpass dichromic mirror and 610/20 emission bandpass filter. Data was gated for cells according to side and forward scatter areas, live cells using the forward scatter area versus PE-Texas Red area, and for single cell events using the forward scatter width versus side scatter area. Replicate numbers correspond to biological replicates.

Flow Cytometry Measurement of COX-2 Activity in RAW 264.7 Macrophages under AneroPack® Hypoxic Conditions. RAW 264.7 macrophage cells (300,000 cells, 2 mL of 150,000 cells/mL) were seeded into 6-well plates and incubated for 48 to 72 h under standard conditions for a final confluency of ~60-80%. The media was removed and replaced with serum-free DMEM (1.98 mL) followed by LPS (1 µg/mL final concentration, 20 µL of 100 µg/mL in PBS) 19 h before collection. Cellular GSH was depleted 2 h prior to collection via treatment with BSO (0.2 mM final concentration, 40 µL 10 mM solution in 1:1 DMSO: serum-free DMEM, 1% DMSO final concentration). Cells were collected by treatment with 0.5 mL 0.25% trypsin-EDTA for less than 5 minutes at 37 ºC and then the trypsin was inactivated with 1.0 mL DMEM media containing 10% FBS. The solution was partitioned for two samples, which were subsequently collected via centrifugation at 6,000 RPM at 4 ºC in 1.6 mL Eppendorf tubes. The media was removed, and cells were resuspended in 0.2 mM BSO with 10 µM CoxFluor (1.0 mL 1.5% DMSO final concentration in degassed serum-free DMEM) and incubated for 90

minutes at 37 ºC in a sealed container either with or without an AneroPack® (Mitsubishi Gas Company). When performing inhibition studies, the aforementioned staining solutions were prepared with 20 μM indomethacin without affecting the final concentration of DMSO. After staining, cells were pelleted in 1.6 mL Eppendorf tubes using the aforementioned procedure and were resuspended in degassed PBS. Samples were stored on ice prior to analysis on a BD LSR Fortessa Flow Cytometry Analyzer with 561 nm excitation and 582/15 emission bandpass filter. Dead cells were excluded from the analysis by staining samples (~300 μL) with propidium iodide (1 μL of 1 mg/mL in deionized water) for 5-10 minutes at room temperature before analysis with 561 nm excitation and 595 nm longpass dichromic mirror and 610/20 emission bandpass filter. Data was gated for live cells the forward scatter higher versus PE-Texas Red area, and for single cell events using the forward scatter width versus side scatter area. Replicate numbers correspond to biological replicates (3 samples of pooled cells on 2 independent days).

Flow Cytometry Measurement of COX-2 Activity in RAW 264.7 Macrophages under Variable Oxygen Concentrations. RAW 264.7 macrophage cells (500,000 cells, 2 mL of 250,000 cells/mL) were seeded into 6-well plates and incubated for 48 h under standard conditions for a final confluency of ~80%. The media was removed and replaced with serum-free DMEM (1.98 mL) followed by LPS (1 μg/mL final concentration, 20 μL of 100 μg/mL in PBS) 19 h before collection. Cellular GSH was depleted 2 h prior to collection via treatment with BSO (0.2 mM final concentration, 40 μL 10 mM solution in 1:1 DMSO: serum-free DMEM, 1% DMSO final concentration). Cells were collected by treatment with 0.5 mL 0.25% trypsin-EDTA for less than 5 minutes at 37 ºC and then the trypsin was inactivated with 1.0 mL DMEM media containing 10% FBS. Three wells were pooled (1.5 mL x 3) for a final volume of 4.5 mL cell suspension before partitioning into three tubes (one tube per oxygen concentration) for centrifugation at 6,000 RPM at 4 ºC in 1.6 mL Eppendorf tubes. The media was removed, and cells were resuspended in 0.2 mM BSO with 10 μM CoxFluor (1.5 mL, 1.5% DMSO final concentration in pre-equilibrated serum-free DMEM, media was equilibrated for ~24 h at the desired oxygen concentration followed by ~ 2 h re-equilibration following the addition of BSO, CoxFluor is added immediately before use prevent any photo-oxidation). The resulting cell suspension was incubated for 90 minutes at 37 ºC under ~21, 1.0, or 0.1% oxygen with 5% CO_2 in an ultra-low cell attachment six well plate (Corning® Costar®) to facilitate rapid oxygen exchange. After staining, cells were pelleted using the aforementioned procedure and were resuspended in PBS. Samples were stored on ice prior to analysis on a BD LSR Fortessa Flow Cytometry Analyzer with 561 nm excitation and 582/15 emission bandpass filter. Dead cells were excluded from the analysis by staining samples (~300 μL) with propidium iodide (1 μL of 1 mg/mL in deionized water) for 5-10 minutes at room temperature before analysis with 561 nm excitation and 595 nm longpass dichromic mirror and 610/20 emission bandpass filter. Data was gated for live cells the forward scatter higher versus PE-Texas Red area, and for single cell events using the forward scatter width versus side scatter area. Replicate numbers correspond to biological replicates (3 sample of pooled cells on 2 independent days).

Enzyme-Linked Immunosorbent Assay (ELISA) for Mouse COX-2. Protein concentration was measured directly from the same samples as the Flow Cytometry Measurement of COX-2 Activity in RAW 264.7 Macrophages under Variable Oxygen Conditions. The ELISA was performed using the SimpleStep ELISA Mouse COX2 ELISA Kit (ab210574, Abcam) according to the manufacturer's protocol. Briefly, cells were washed with cold PBS (1.0 mL × 2) prior to lysis in cold 1X Cell Extraction Buffer PTR on ice for 20 minutes. The debris was removed via centrifugation at 18,000 x g for 20 minutes at 4 ºC and the supernatants were collected and stored at -80 ºC prior to use. Protein concentration was measured using the BCA Assay (Thermo Fisher Scientific) according to the manufacturer's protocol and the lysate was diluted with 1X Cell Extraction Buffer PTR for a final concentration of 25 μg/mL total protein. Cell lysate (50 μL) and then Antibody Cocktail (50 μL) were added to each well in duplicate and the sealed plate was incubated with vigorous shaking (400 rpm) for 1 h at 22 ºC. After binding, each well was washed thoroughly with 1X Wash Buffer PT (350 μL × 3). TMB Substrate (100 μL) was allowed to incubate in the dark with vigorous stirring for 10 minutes at 22 ºC before quenching with Stop Solution (100 μL). The optical density was measured at 450 nm and the protein concentration was interpolated according to a standard curved (prepared in duplicate). Protein concentrations are reported for the COX-2 concentration in a 25 μg/mL total protein stock.

Results and Discussion

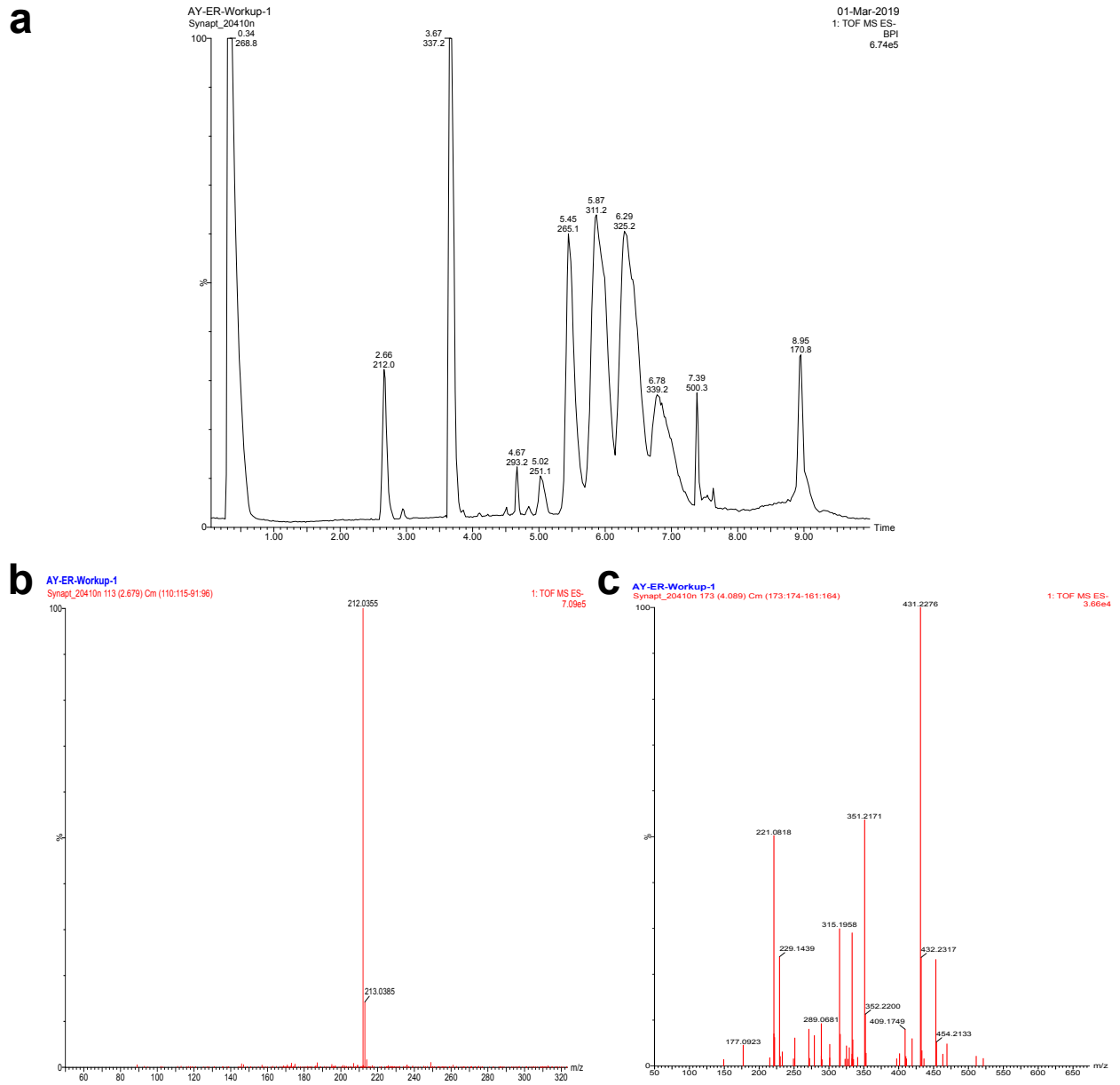

Figure S1. (a) LC-HRMS analysis of the crude reaction between CoxFluor (10 μM), COX-2 (250 nM), and hemin (1 μM) in 100 mM Tris-HCl buffer (pH 8.0). The products were extracted with EtOAc after incubation at room temperature for 4 h and the organic layer was concentrated under vacuum. Products were separated on a CORTECS™ UPLC C18 column (1.6 μm, 2.1 by 50 mm) with a linear gradient using a combination of solvent A (95% water, 5% acetonitrile, 0.1% TFA) and solvent B (95% acetonitrile, 5% water, 0.1% TFA) at a flow rate of 0.5 mL/minute. Gradient protocol in minutes: 0 - 0.5 (100% A); 0.5 -6 (20% A); 6 – 8 (100% B); 8 – 8.1 (80% A); and 8.1 – 10 (80% A). High resolution spectra for (b) resorufin (HRMS [M - H]$^-$ calc'd mass for $C_{12}H_6NO_3$ = 212.0348, found = 212.0355) and (c) PGG_2 (HRMS [M - H]$^-$ calc'd mass for $C_{20}H_{31}NO_5$ = 351.2171, found = 351.2171) were observed.

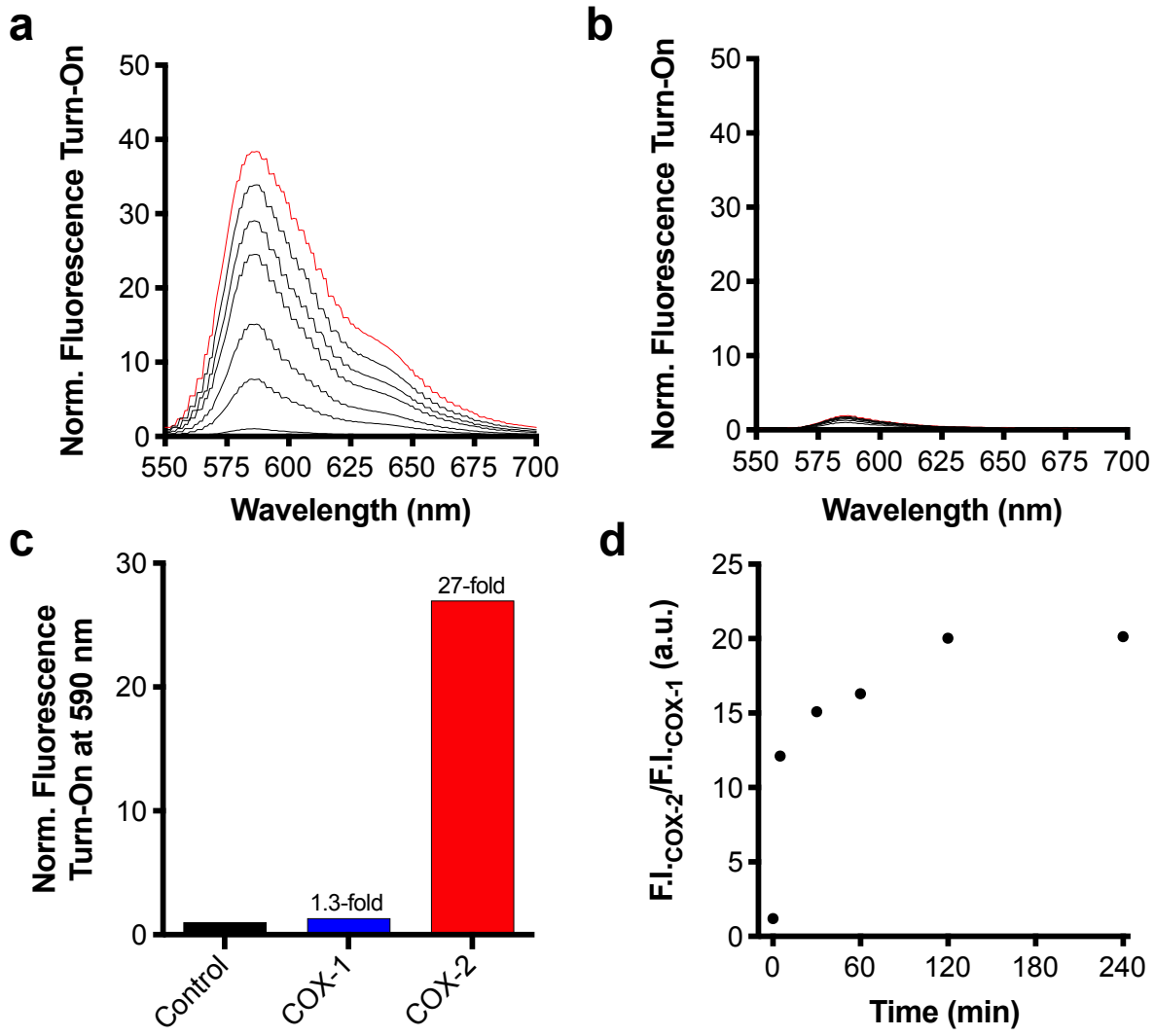

Figure S2. Representative time-course of CoxFluor fluorescence spectra after treatment with (a) COX-2 or (b) COX-1 over 4 h (red line indicates final time point, normalized to initial timepoint). (c) Comparison of final fluorescence intensity at 590 nm for CoxFluor treated with COX-2 (red) or COX-1 (blue) relative to a buffer control (black). (d) Relative selectivity for COX-2 over COX-1 as a function of time. Reactions were performed at room temperature using the fluorimeter assay protocol (submicroquartz cuvettes) with 10 mM CoxFluor and 250 nM enzyme (COX-1 specific activity is 1.3-fold greater than COX-2 at this concentration) in 100 mM Tris-HCl (pH 8.0).

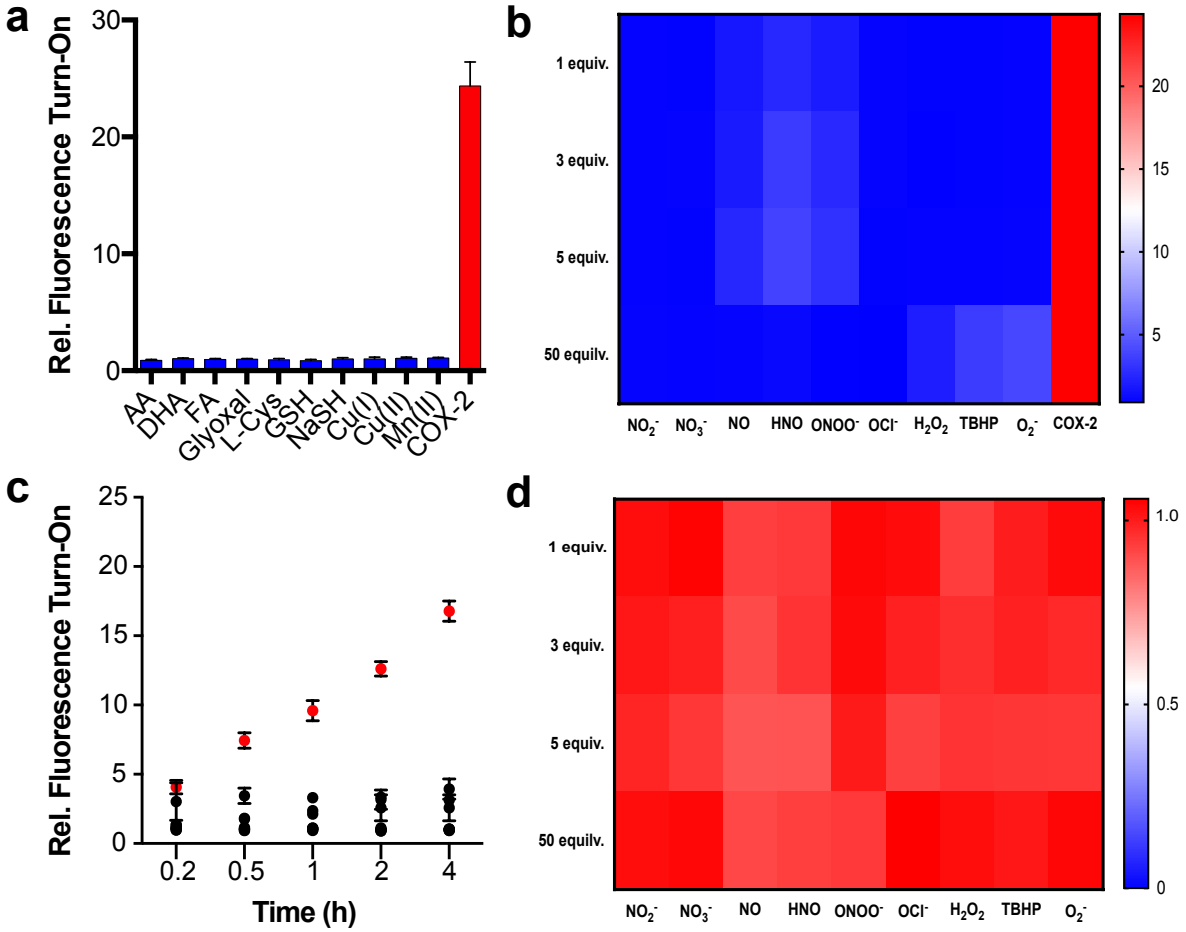

Figure S3. (a) CoxFluor response to reactive carbonyl (AA: ascorbic acid; DHA: dehydroascorbic acid; FA: formaldehyde; glyoxal), reactive thiols (L-cysteine; GSH: reduced glutathione; NaSH), and metal species (500 μM). (b) Heat map of the mean fluorescence enhancement of CoxFluor following treatment with 1, 3, 5, or 50 equivalents of RNS or ROS. (c) Representative time course of the relative turn on for COX-2 (250 nM, red) compared to a range of ROS and RNS (5 equivalents). The same was observed for all other analyte equivalents. (d) Stability of resorufin in the presence of 1, 3, 5, and 50 equivalents of ROS and RNS. Fluorescence enhancements were measured for CoxFluor or resorufin (10 μM) using the plate reader assay. Endpoint assays were performed at 4 h and the fluorescence enhancement was calculated relative to a buffer control (100 mM Tris-HCl, pH 8.0) at the corresponding time point. Values are reported as the mean ± standard deviation (*n* = 3).

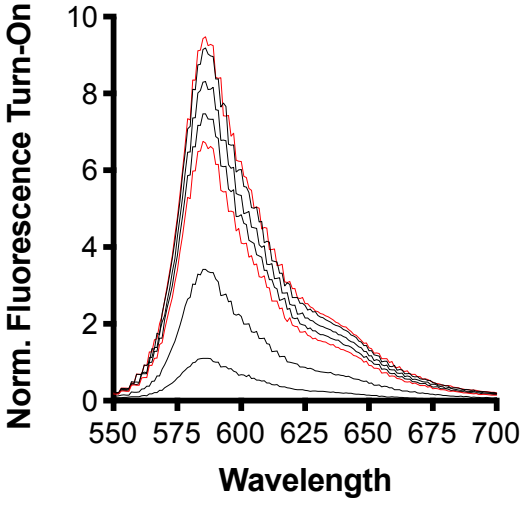

Figure S4. Relative fluorescence for CoxFluor (10 μM) incubated with COX-2 (250 nM), GSH (1 mM) and hemin (1 μM) over the course of 4 h at room temperature in 100 mM Tris HCl buffer (pH 8.0). Assay was performed according to the fluorimeter assay.

SUPPORTING INFORMATION

Table S1: Calculated root-mean-standard-deviation (RMSD, in Å) for the selected structure of COX-1 (PDB ID: 5U6X) compared to a panel of other structures in the protein databank.

PDB	***Alpha Carbons***	***Backbone***	***Heavy***
1PRH[37]	0.15	0.16	0.32
1PTH[38]	0.13	0.15	0.28
1PGE[39]	0.13	0.15	0.28
1PGF[39]	0.13	0.15	0.28
1PGG[39]	0.13	0.14	0.28
1CQE[37]	0.18	0.18	0.34
1EBV[40]	0.17	0.19	0.37
1DIY[33]	0.17	0.19	0.33
1EQG[41]	0.16	0.17	0.33
1EQH[41]	0.16	0.17	0.32
1HT5[41]	0.20	0.22	0.38
1HT8[41]	0.19	0.20	0.36
1FE2[42]	0.17	0.19	0.33
1IGX[43]	0.18	0.20	0.32
1IGZ[43]	0.16	0.18	0.32
1Q4G[44]	0.20	0.21	0.42
1U67[45]	0.18	0.19	0.32
2AYL[46]	0.19	0.19	0.41
2OYE[47]	0.18	0.19	0.32
2OYU[47]	0.16	0.18	0.34
3KK6[48]	0.19	0.22	0.31
3N8V[49]	0.18	0.20	0.36
3N8W[49]	0.18	0.19	0.37
3N8X[49]	0.23	0.24	0.44
3N8Y[49]	0.22	0.23	0.40
3N8Z[49]	0.21	0.2	0.42
4O1Z[50]	0.18	0.19	0.39
5WBE[18]	0.09	0.10	0.19

SUPPORTING INFORMATION

Table S2: Calculated RMSD (Å) for the selected structure of COX-2 (PDB ID: 5KIR) compared to a panel of other structures in the protein databank.

PDB	***Alpha Carbons***	***Back Bone***	***Heavy***
1DDX[51]	0.15	0.17	0.28
1PXX[52]	0.17	0.18	0.30
3KRK[6]	0.21	0.21	0.44
3LN0[53]	0.12	0.14	0.28
3LN1[53]	0.14	0.15	0.27
3MQE[53]	0.32	0.34	0.50
3NT1[54]	0.20	0.20	0.43
3NTB[54]	0.18	0.19	0.46
3NTG[53]	0.19	0.20	0.39
3OLT[55]	0.24	0.25	0.41
3OLU[55]	0.23	0.24	0.42
3Q7D[56]	0.22	0.25	0.47
3RR3[56]	0.12	0.14	0.24
3TZI[57]	0.23	0.23	0.47
4FM5[58]	0.15	0.20	0.36
4M10[50]	0.18	0.19	0.39
4M11[50]	0.19	0.21	0.49
4OTJ[59]	0.17	0.18	0.38
4OTY[60]	0.23	0.24	0.43
4PH9[61]	0.20	0.20	0.43
4RRW[62]	0.15	0.15	0.28
4RRX[62]	0.20	0.20	0.38
4RRY[62]	0.19	0.21	0.41
4RRZ[62]	0.15	0.15	0.28
4RS0[62]	0.23	0.23	0.42
4RUT[63]	0.18	0.19	0.40
4Z0L[64]	0.18	0.18	0.33
5F19[65]	0.22	0.22	0.43
5F1A[65]	0.20	0.20	0.43
5FDQ[65]	0.20	0.21	0.44
5IKQ[66]	0.18	0.19	0.42
5IKR[66]	0.20	0.20	0.42
5IKT[66]	0.15	0.16	0.36
5IKV[66]	0.15	0.16	0.38
5W58[67]	0.23	0.23	0.41
6BL3[68]	0.13	0.14	0.27
6BL4[68]	0.15	0.16	0.31

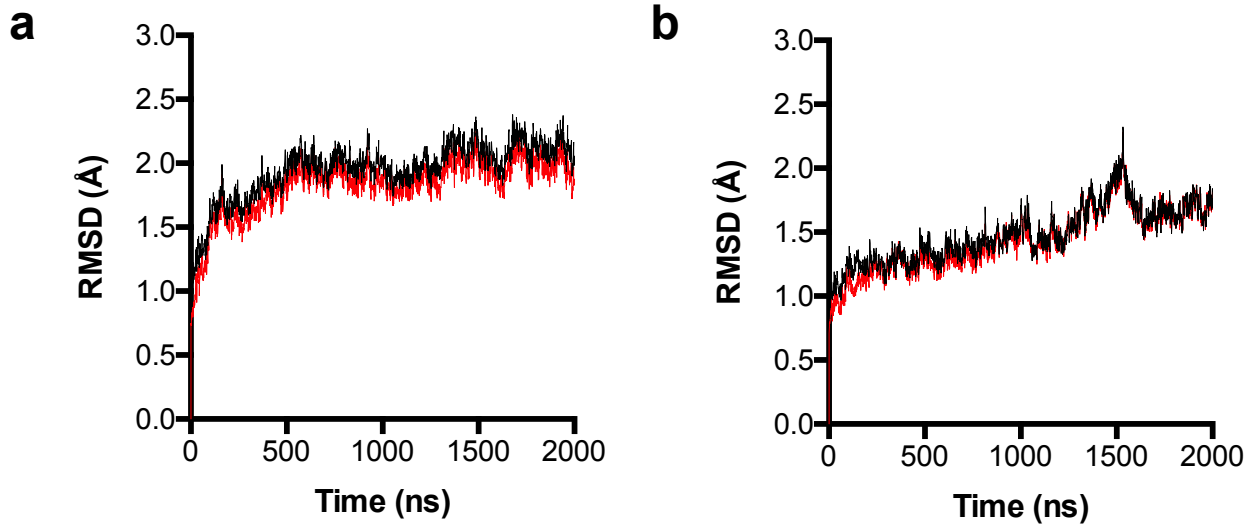

Figure S5. RMSD of simulated (a) COX-1 and (b) COX-2 versus the initial crystal structure (PDB 5U6X or 5KIR) as a function of simulation time. Monomer A and B are plotted as black and red lines, respectively.

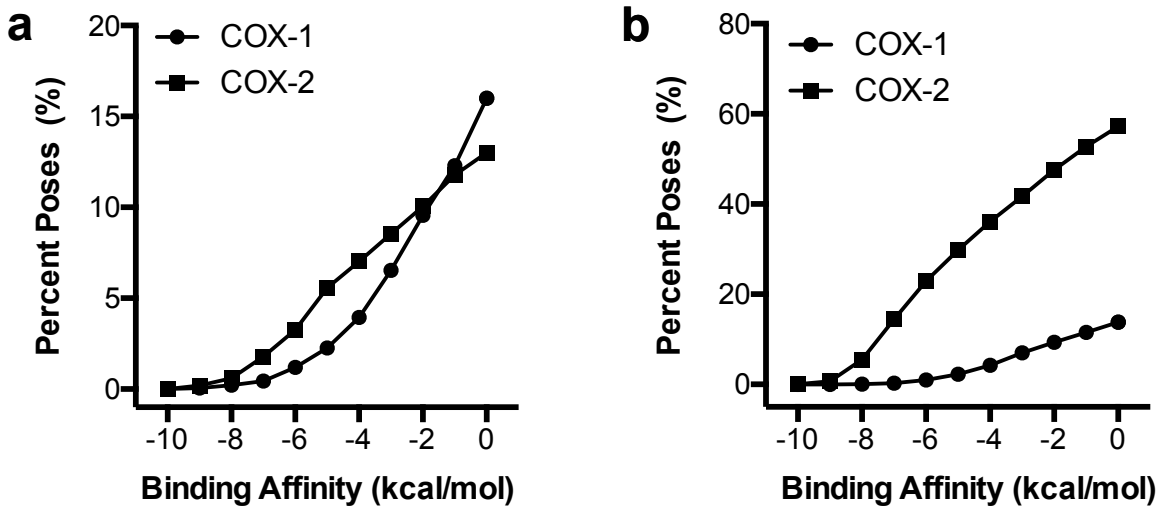

Figure S6. Percent of the total docked poses of CoxFluor bound within the (a) cyclooxygenase and (b) peroxidase active sites of COX-2 at a particular Vina AutoDock docking score binding affinity.

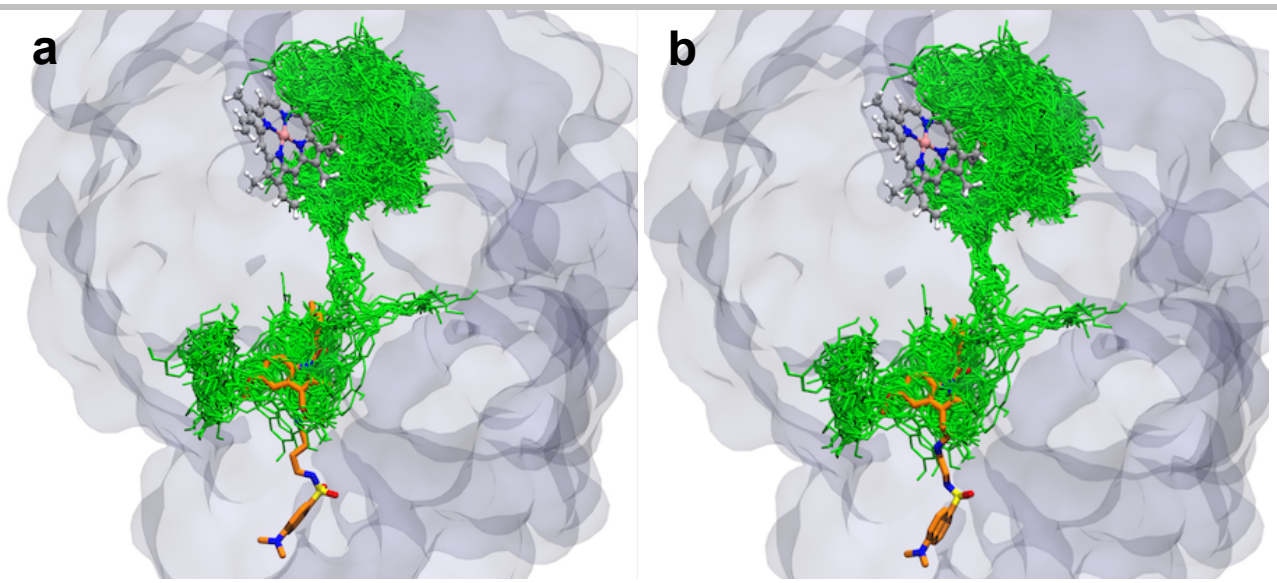

Figure S7. Comparison between CoxFluor (green, -7 kcal/mol docking score cutoff) bound to COX-2 and dansyl-conjugated indomethacin either (a) without (PDB 6BL3) or (b) with a *n*-butyl-diamine linker (PDB 6BL4).[68]

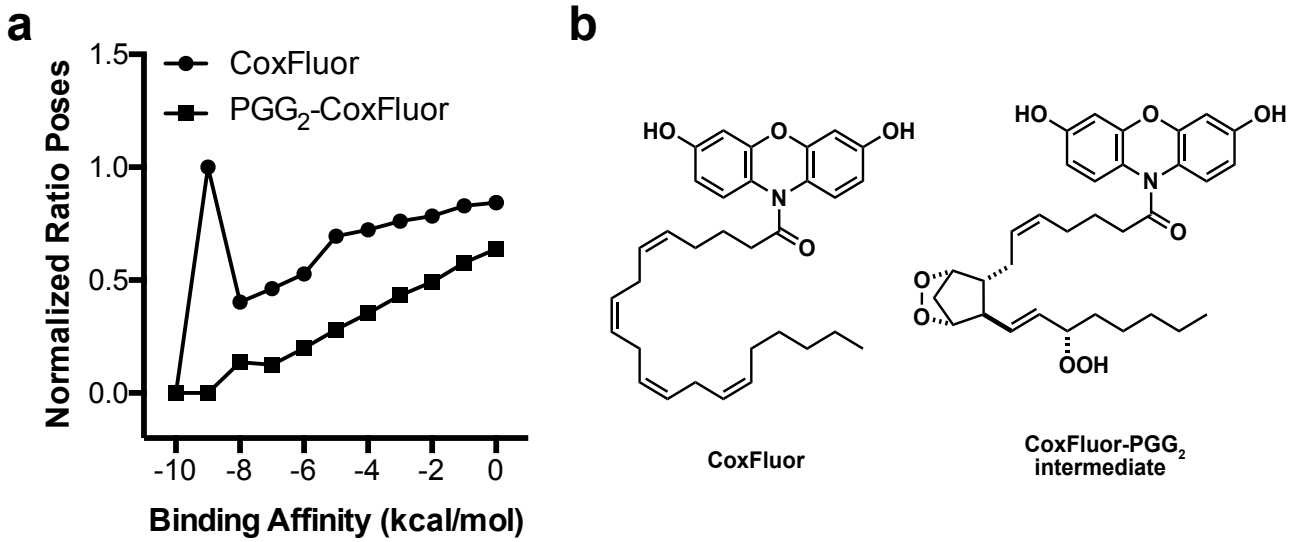

Figure S8. (a) Normalized ratio of cyclooxygenase to peroxidase binding modes for CoxFluor and PGG_2-CoxFluor intermediate. (b) Structures of CoxFluor and CoxFluor-PGG_2 intermediate.

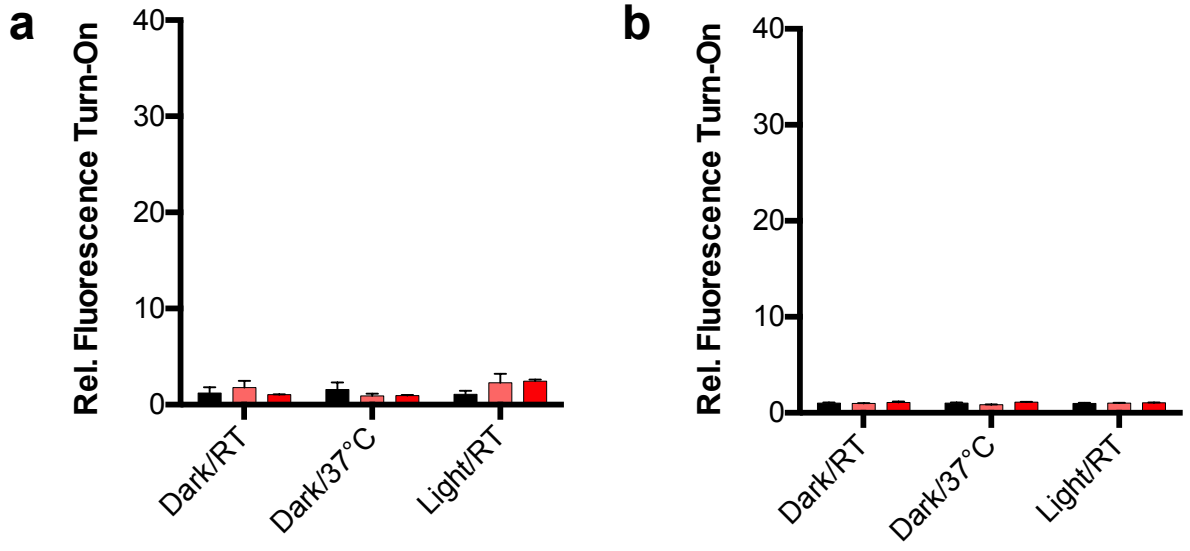

Figure S9. Stability of (a) CoxFluor and (b) resorufin in Tris-HCl (100 mM, pH 8.0, black) and serum-free DMEM (light red), DMEM with 10% FBS (red) after 8 h at room temperature with or without exposure to ambient light. Values are reported as the mean ± standard deviation (*n* = 3).

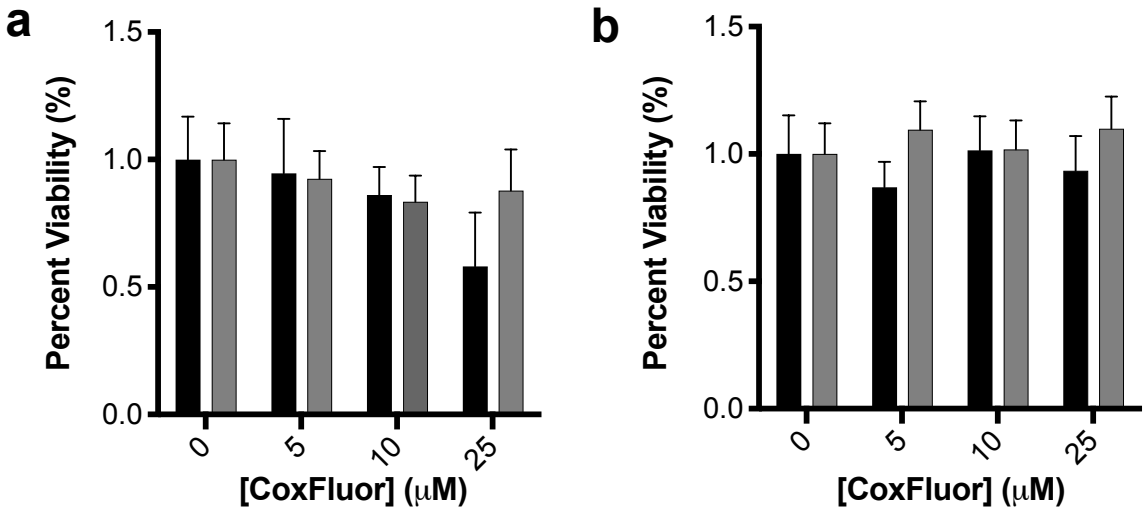

Figure S10. Cell viability for CoxFluor in (a) HEK 293T cells and (b) RAW 264.7 macrophage cells after 6 h incubation as measured by the trypan blue exclusion assay (black) and MTT assay (grey). Values are reported as the mean ± standard deviation (*n* = 3).

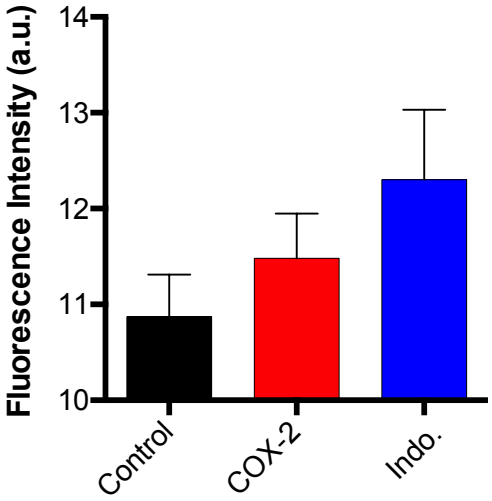

Figure S11. Quantified confocal imaging of COX-2 activity after 3 h incubation in either non-transfected (control) or transfected HEK 293T cells. Indomethacin inhibition (Indo, 10 μM) was performed in transfected cells. Values are reported as the mean ± standard deviation (*n* = 3).

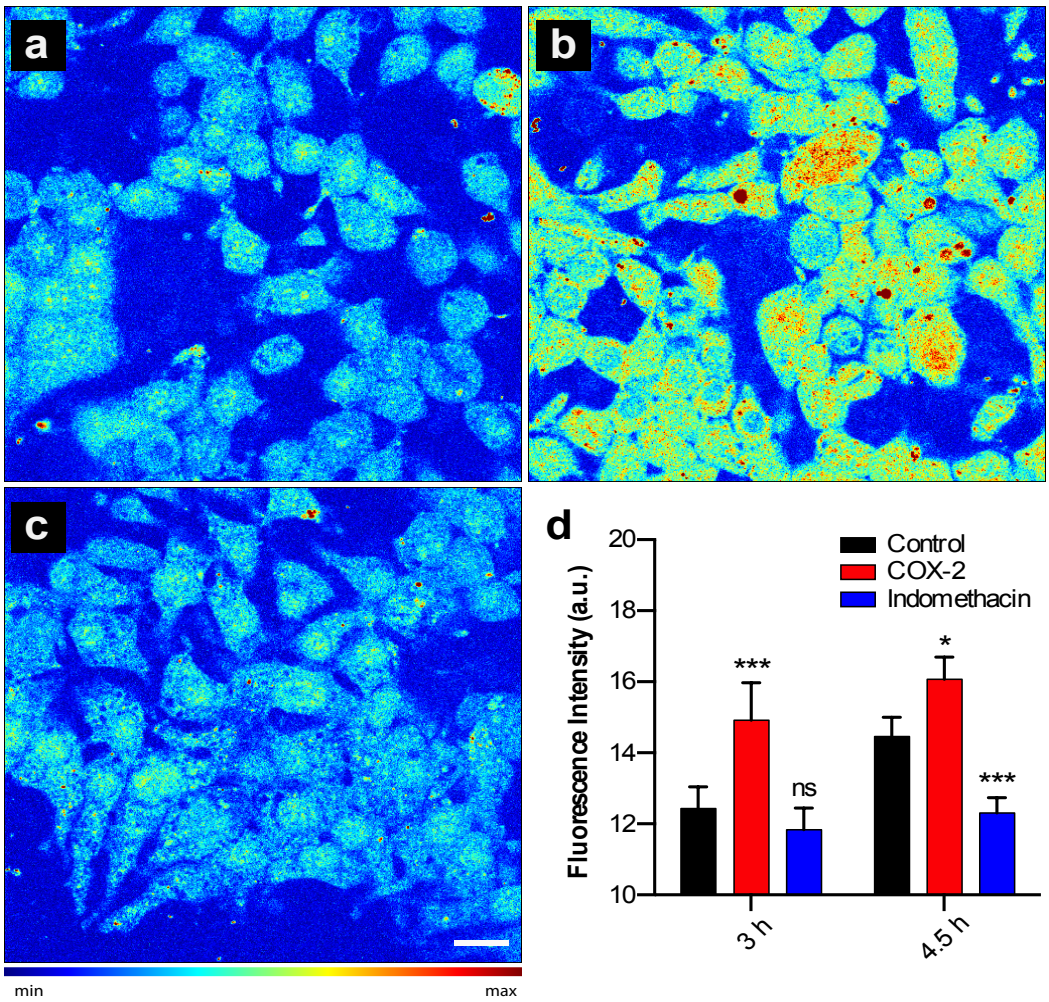

Figure S12. Confocal imaging of COX-2 activity in (a) control, (b) transfected, and (c) indomethacin-treated transfected HEK 293T cells after 3-4.5 h incubation with CoxFluor (10 μM) at 37 ºC following a 0.5 h NEM (1 mM) treatment. Scale bar (white) represents 10 μm. (d) Quantification of images. Values are reported as the mean ± standard deviation (*n* = 3). Statistical analysis was performed using 2-way ANOVA (α = 0.05). Fluorescence intensities were compared to the control at each time point using Sidak's multiple comparison test (α = 0.05). *, $p < 0.05$; ***, $p < 0.001$.

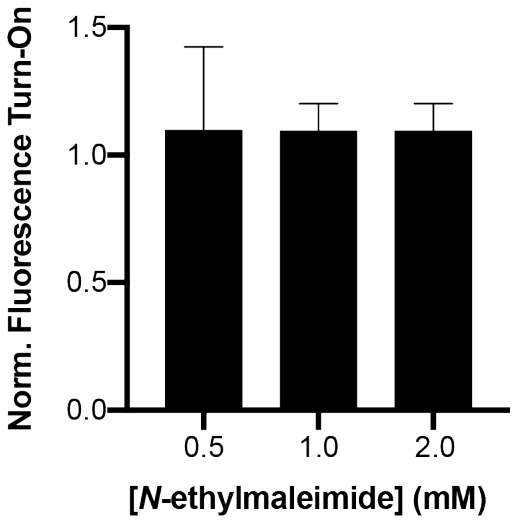

Figure S13. Normalized fluorescence response for CoxFluor (10 μM) after incubation with COX-2 (250 nM) at varying concentrations of *N*-ethylmaleimide. Samples were incubated at room temperature for 4 h and normalized to the fluorescence with 0 mM *N*-ethylmaleimide. Assay was performed according to the plate reader assay. Values are reported as the mean ± standard deviation (*n* = 3).

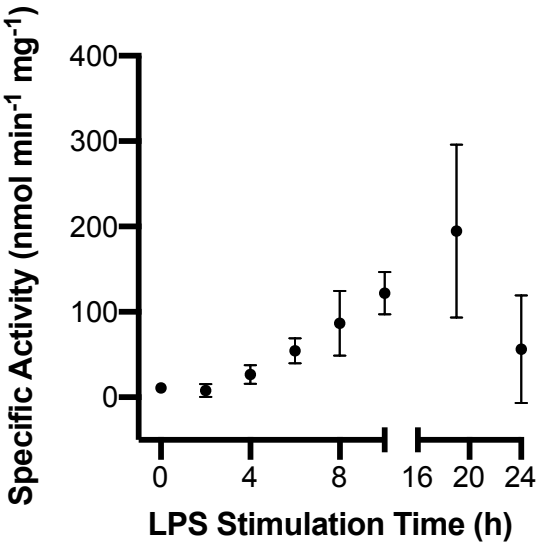

Figure S14. RAW 264.7 macrophage cell lysate COX-2 activity as a function of LPS stimulation time. Enzymatic activity was measured at room temperature with CoxFluor (10 μM) in 89 mM Tris-HCl buffer (pH 8.0) containing 10% CelLytic M and 1 mM N-ethylmaleimide. Initial rates were measured within the linear region (typically the first 30 seconds) and protein concentration was measured using the BCA assay. Values are reported as the mean ± standard deviation (*n* = 3).

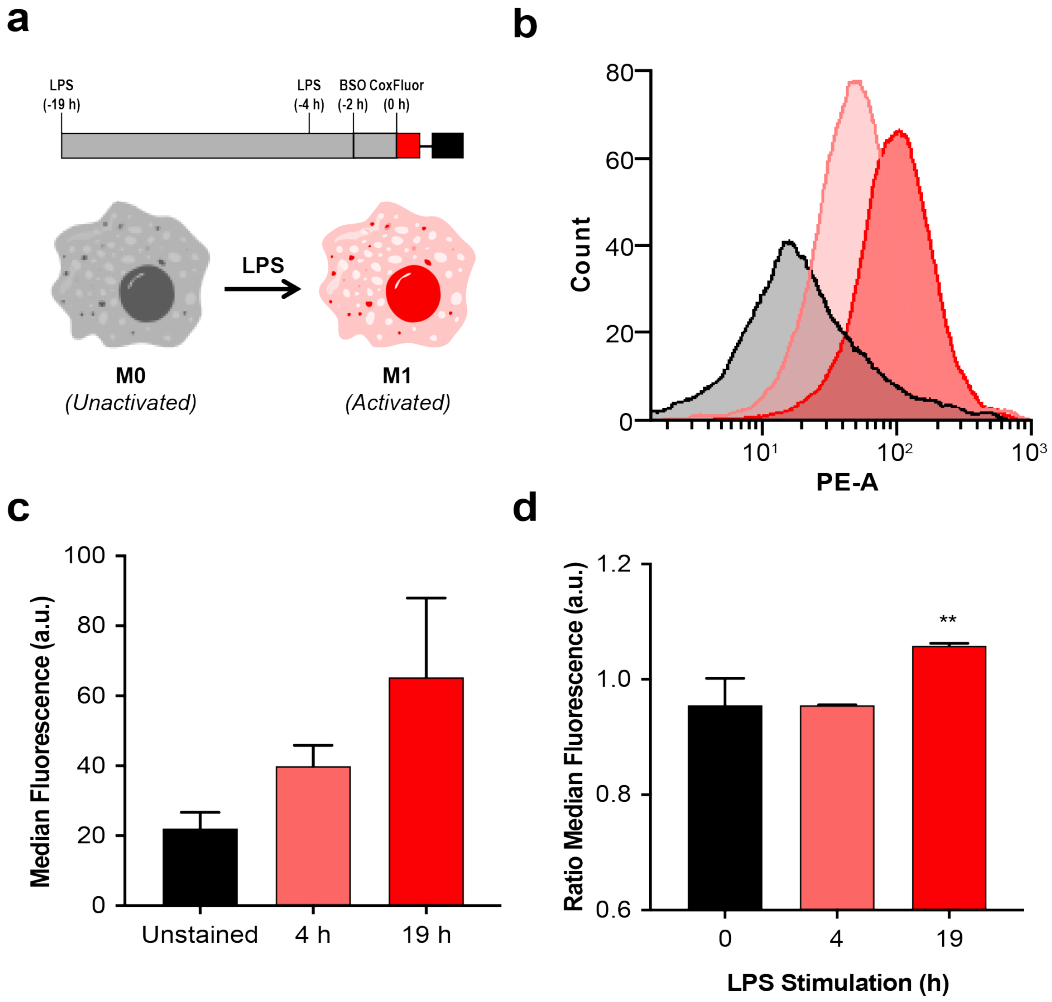

Figure S15. (a) A schematic for measuring the time-dependent changes in LPS-activated RAW 264.7 macrophage cells with flow cytometry. (b) Representative histogram and (c) quantified median fluorescence for unstained (black), and CoxFluor stained cells after 4 (salmon) and 19 h (red) LPS activation. (d) Quantified ratio of median fluorescence between cells stained with CoxFluor to cells stained with CoxFluor in the presence of indomethacin (20 μM). All staining was performed with 10 μM CoxFluor, 200 μM BSO was added 2 h prior to staining, and values are reported as the mean ± standard deviation (n = 3). Statistical analysis was performed using a 2-way ANOVA (α = 0.05) with Tukey's multiple t test (α = 0.05) for comparison of 19 h LPS- stimulation to both 0 and 4 h. **, $p < 0.01$.

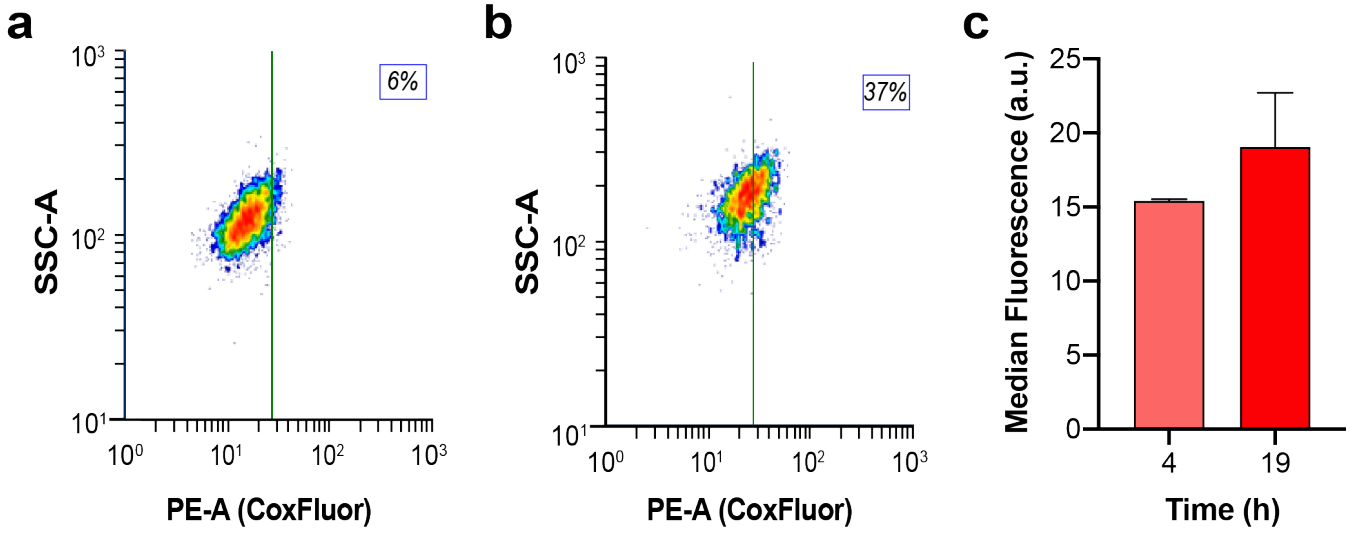

Figure S16. Representative density plot for LPS-activated RAW 264.7 macrophage cells with flow cytometry without BSO with (a) 4 h or (b) 19 h LPS-stimulation. (c) Quantified median fluorescence for CoxFluor (10 μM) stained cells after 4 (salmon) and 19 h (red) LPS activation. Percentages indicate the percent COX-2 positive cells, as defined by the green line. Values are reported as the mean ± standard deviation (n = 3).

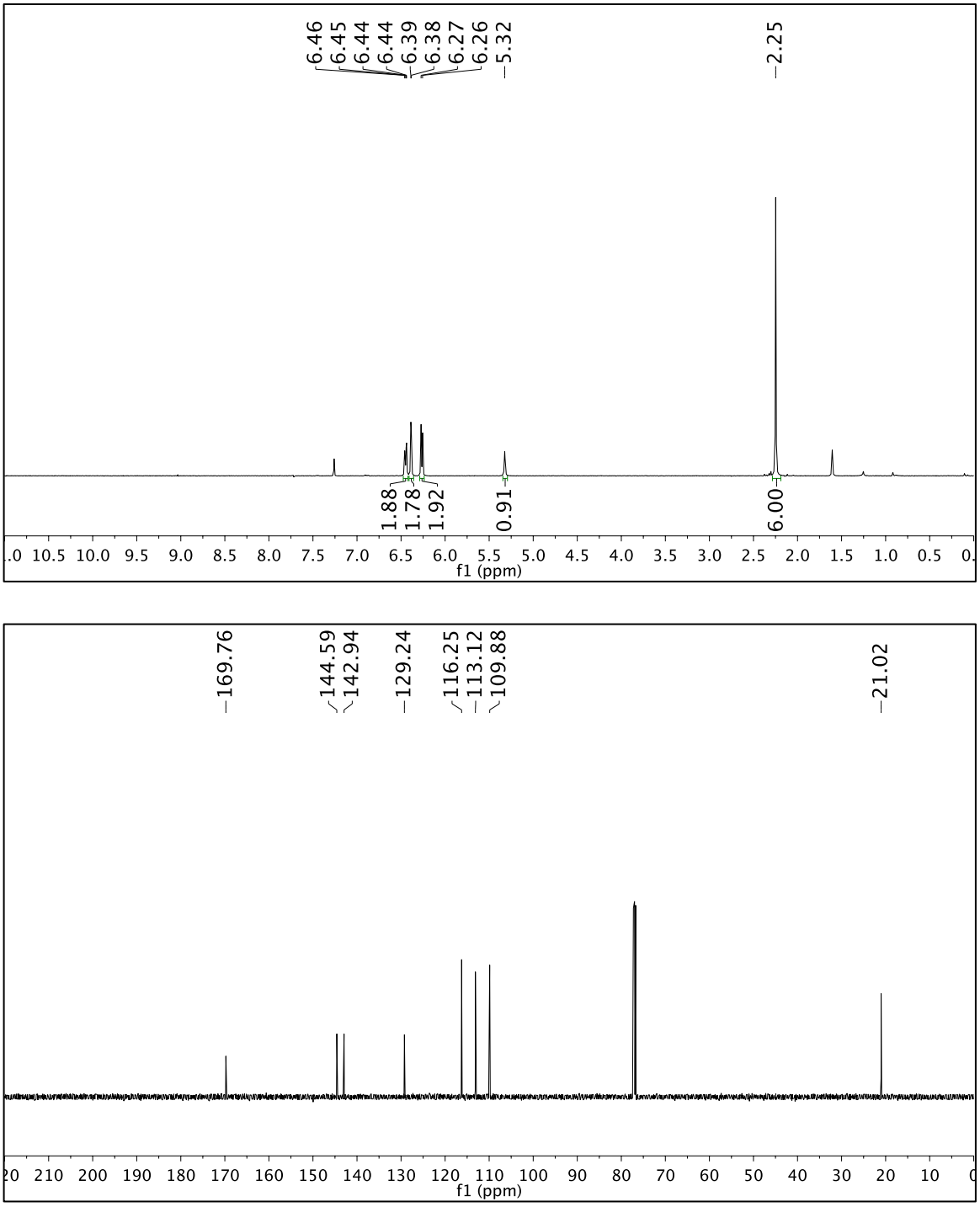

Figure S16. (top) ^{1}H NMR (500 MHz, $CDCl_3$) and (bottom) ^{13}C NMR (125 MHz, $CDCl_3$) spectra of **1**.

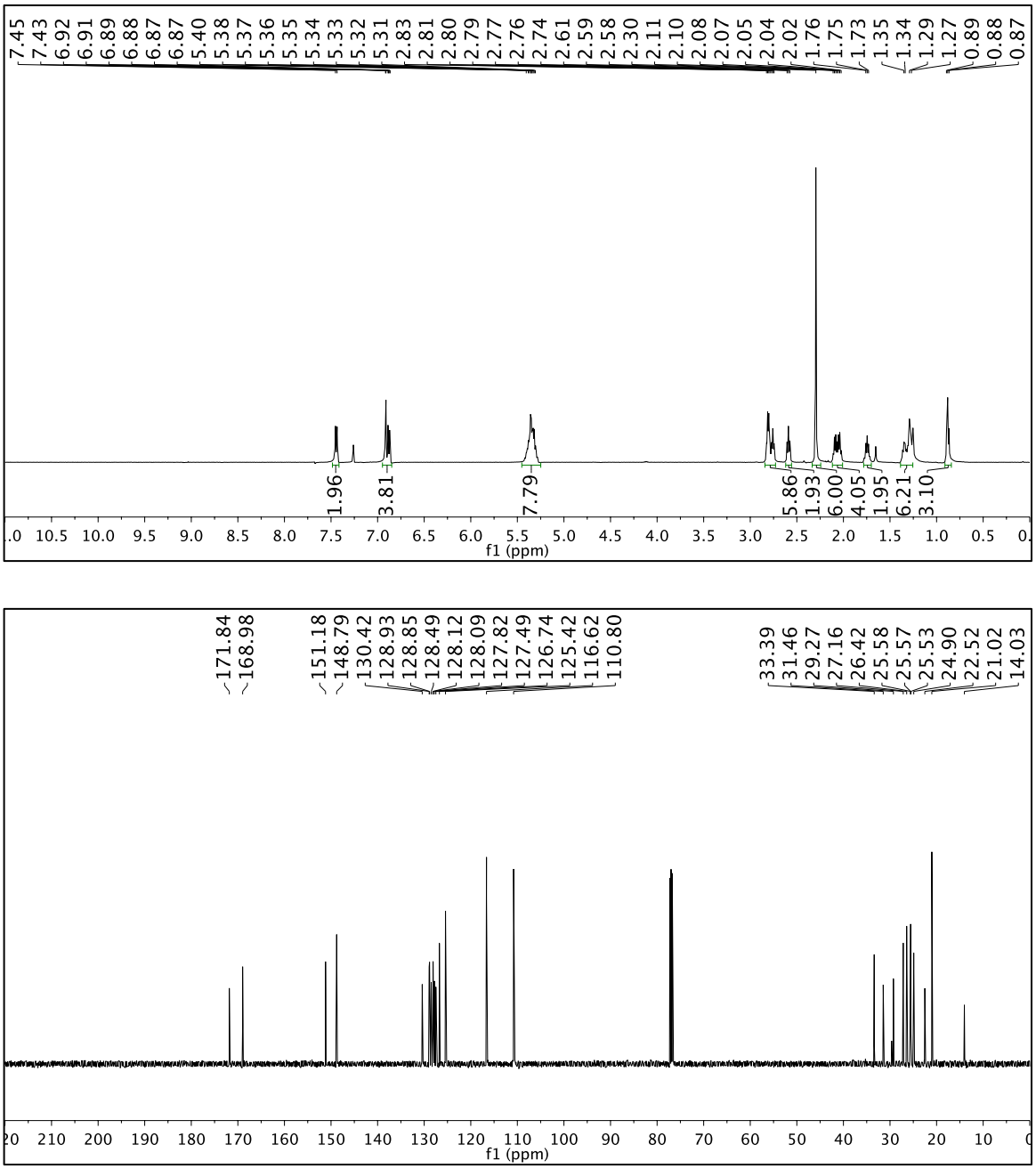

Figure S17. (top) ^{1}H NMR (500 MHz, $CDCl_3$) and (bottom) ^{13}C NMR (125 MHz, $CDCl_3$) spectra of **2.**

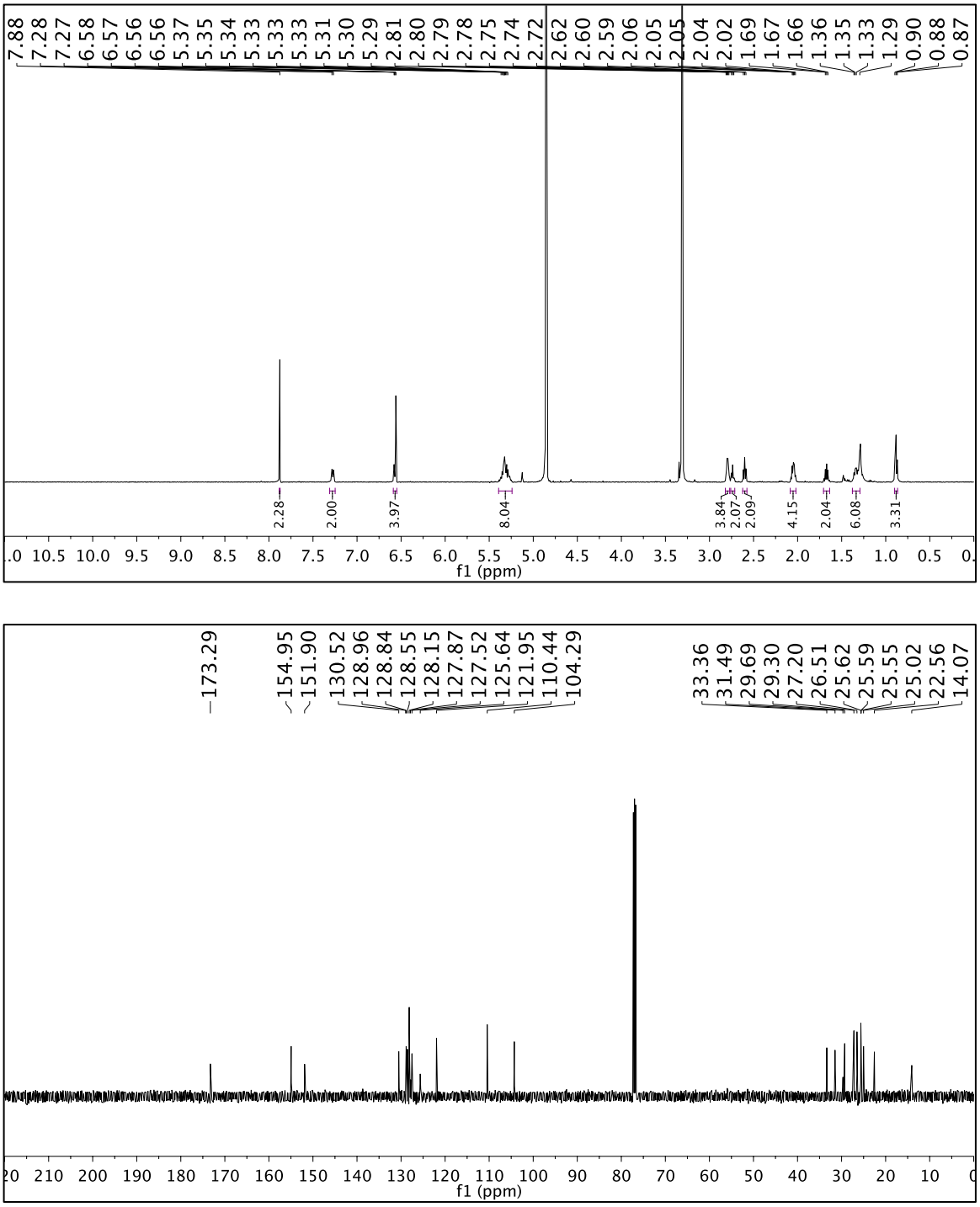

Figure S18. (top) ^{1}H NMR (500 MHz, CD_3OD) and (bottom) ^{13}C NMR (125 MHz, $CDCl_3$) spectra of **CoxFluor.**

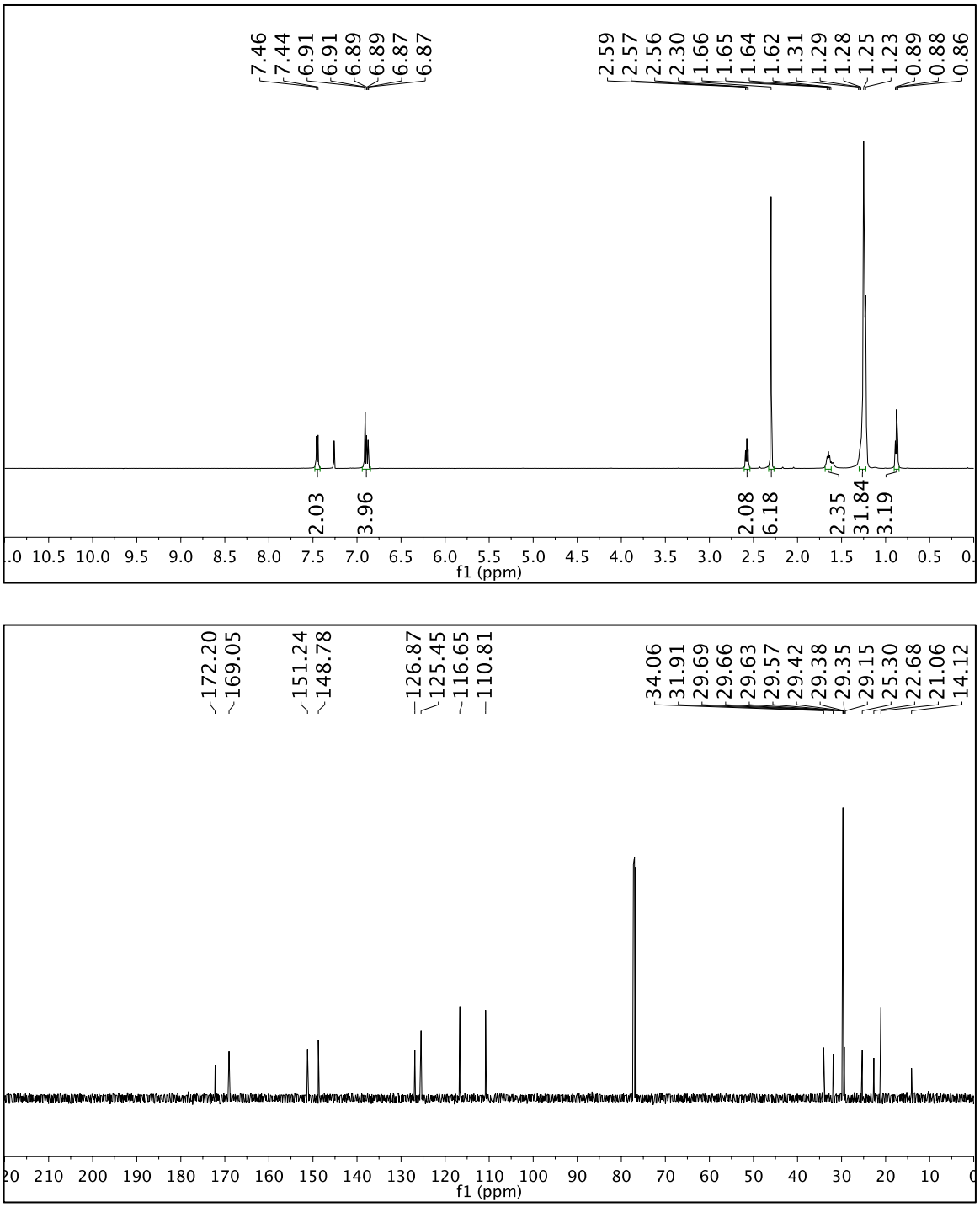

Figure S19. (top) ^{1}H NMR (500 MHz, $CDCl_3$) and (bottom) ^{13}C NMR (125 MHz, $CDCl_3$) spectra of **3**.

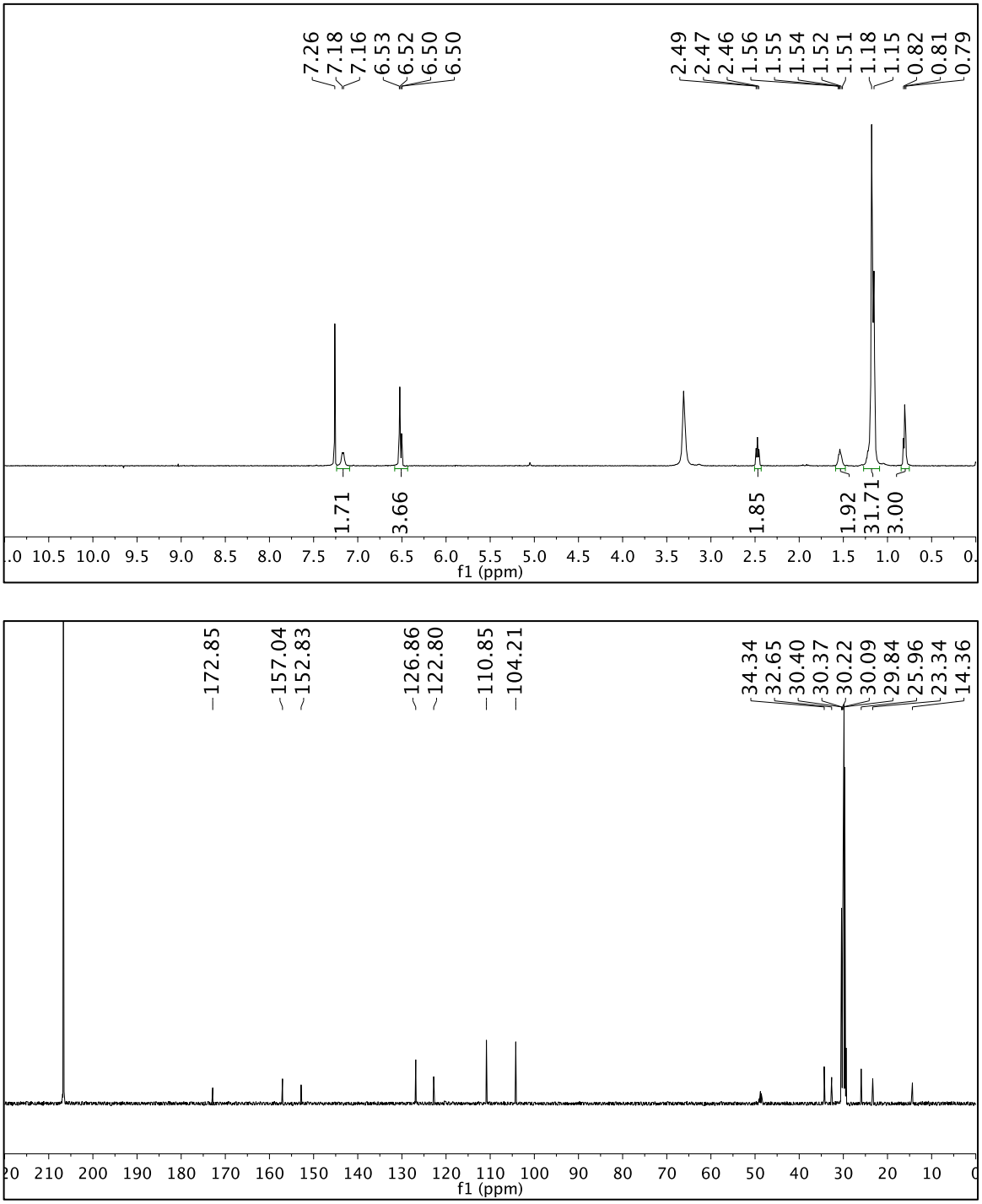

Figure S20. (top) ^{1}H NMR (500 MHz, $CDCl_3$) and (bottom) ^{13}C NMR (125 MHz, $(CD_3)_2CO$) spectra of Ctrl-CoxFluor.

References

[1] C. A. Schneider, W. S. Rasband, K. W. Eliceiri, *Nat. Methods* **2012**, *9*, 671–5.
[2] Y. Hitomi, T. Takeyasu, T. Funabiki, M. Kodera, *Anal. Chem.* **2011**, *83*, 9213–9216.
[3] S. M. Sagnella, C. E. Conn, I. Krodkiewska, X. Mulet, C. J. Drummond, *Soft Matter* **2011**, *7*, 5319–5328.
[4] C. Würth, M. Grabolle, J. Pauli, M. Spieles, U. Resch-Genger, *Nat. Protoc.* **2013**, *8*, 1535–1550.
[5] F. L. Arbeloa, P. R. Ojeda, I. L. Arbeloa, *J. Lumin.* **1989**, *44*, 105–112.
[6] A. J. Vecchio, D. M. Simmons, M. G. Malkowski, *J. Biol. Chem.* **2010**, *285*, 22152–22163.
[7] B. J. Orlando, D. R. McDougle, M. J. Lucido, E. T. Eng, L. A. Graham, C. Schneider, D. L. Stokes, A. Das, M. G. Malkowski, *Arch. Biochem. Biophys.* **2014**, *546*, 33–40.
[8] B. J. Orlando, P. P. Borbat, E. R. Georgieva, J. H. Freed, M. G. Malkowski, *Biochemistry* **2015**, *54*, 7309–7312.
[9] R. J. Kulmacz, W. E. M. Lands, *Prostaglandins* **1985**, *29*, 175–190.
[10] T. Miyamoto, N. Oging, S. Yamamoto, O. Hayaishi, *J. Biol. Chem.* **1976**, *251*, 2629–2636.
[11] D. R. McDougle, A. Palaria, E. Magnetta, D. D. Meling, A. Das, *Protein Sci.* **2013**, *22*, 964–979.
[12] H. C. Huff, D. Maroutsos, A. Das, *Protein Sci.* **2019**, *28*, 928–940.
[13] S. Zelasko, A. Palaria, A. Das, *Protein Expr. Purif.* **2013**, *92*, 77–87.
[14] A. L. Shen, T. D. Porter, T. E. Wilson, C. B. Kasper, *J. Biol. Chem.* **1989**, *264*, 7584–7589.
[15] E. Gasteiger, A. Gattiker, C. Hoogland, I. Ivanyi, R. D. Appel, A. Bairoch, *Nucleic Acids Res.* **2003**, *31*, 3784–3788.
[16] M. N. Hughes, R. Cammack, *Methods Enzymol.* **1999**, *301*, 279–287.
[17] R. M. Uppu, *Anal. Biochem.* **2006**, *354*, 165–168.
[18] G. Cingolani, A. Panella, M. G. Perrone, P. Vitale, G. Di Mauro, C. G. Fortuna, R. S. Armen, S. Ferorelli, W. L. Smith, A. Scilimati, *Eur. J. Med. Chem.* **2017**, *138*, 661–668.
[19] B. J. Orlando, M. G. Malkowski, *Acta Crystallogr. Sect. F Struct. Biol. Commun.* **2016**, *72*, 772–776.
[20] R. Maiti, G. H. Van Domselaar, H. Zhang, D. S. Wishart, *Nucleic Acids Res.* **2004**, *32*, W590–W594.
[21] L. N. Carnevale, A. S. Arango, W. R. Arnold, E. Tajkhorshid, A. Das, *Biochemistry* **2018**, *57*, 6489–6499.
[22] M. L. Starr, R. P. Sparks, A. S. Arango, L. R. Hurst, Z. Zhao, M. Lihan, J. L. Jenkins, E. Tajkhorshid, R. A. Fratti, *J. Biol. Chem.* **2019**, *294*, 3100–3116.
[23] J. C. Phillips, R. Braun, W. Wang, J. Gumbart, E. Tajkhorshid, E. Villa, C. Chipot, R. D. Skeel, L. Kalé, K. Schulten, *J. Comput. Chem.* **2005**, *26*, 1781–1802.
[24] J. Huang, S. Rauscher, G. Nawrocki, T. Ran, M. Feig, B. L. De Groot, H. Grubmüller, A. D. MacKerell, *Nat. Methods* **2017**, *14*, 71–73.
[25] S. E. Feller, Y. Zhang, R. W. Pastor, B. R. Brooks, *J. Chem. Phys.* **1995**, *103*, 4613–4621.
[26] G. J. Martyna, D. J. Tobias, M. L. Klein, *J. Chem. Phys.* **1994**, *101*, 4177–4189.
[27] T. Darden, D. York, L. Pedersen, *J. Chem. Phys.* **1993**, *98*, 10089–10092.
[28] U. Essmann, L. Perera, M. L. Berkowitz, T. Darden, H. Lee, L. G. Pedersen, *J. Chem. Phys.* **1995**, *103*, 8577–8593.
[29] S. Miyamoto, P. A. Kollman, *J. Comput. Chem.* **1992**, *13*, 952–962.
[30] W. A. K. Humphrey Dalke Schulten, *J. Mol. Graph.* **1996**, *14*, 33–38.
[31] N. Michaud-Agrawal, E. J. Denning, T. B. Woolf, O. Beckstein, *J. Comput. Chem.* **2011**, *32*, 2319–2327.
[32] R. J. Gowers, M. Linke, J. Barnoud, T. J. E. Reddy, M. N. Melo, S. L. Seyler, J. Domański, D. L. Dotson, S. Buchoux, M. Kenney, Ian, et al., *Proc. 15th Python Sci. Conf.* **2016**, 98–105.
[33] M. G. Malkowski, S. L. Ginell, W. L. Smith, R. M. Garavito, *Science* **2000**, *289*, 1933–1937.
[34] O. Trott, A. J. Olson, *J. Comput. Chem.* **2010**, *31*, 455–461.
[35] E. Roberts, J. Eargle, D. Wright, Z. Luthey-Schulten, *BMC Bioinformatics* **2006**, *7*, 382.
[36] H. Chen, W. Cai, E. S. H. Chu, J. Tang, C. C. Wong, S. H. Wong, W. Sun, Q. Liang, J. Fang, Z. Sun, et al., *Oncogene* **2017**, *36*, 4415–4426.
[37] D. Picot, P. J. Loll, R. M. Garavito, *Nature* **1994**, *367*, 243–249.
[38] P. J. Loll, D. Picot, R. M. Garavito, *Nat. Struct. Mol. Biol.* **1995**, *2*, 637–643.
[39] P. J. Loll, D. Picot, O. Ekabo, R. M. Garavito, *Biochemistry* **1996**, *35*, 7330–7340.
[40] P. J. Loll, C. T. Sharkey, S. J. O'Connor, C. M. Dooley, E. O'Brien, M. Devocelle, K. B. Nolan, B. S. Selinsky, D. J. Fitzgerald, *Mol. Pharmacol.* **2001**, *60*, 1407–1413.
[41] B. S. Selinsky, K. Gupta, C. T. Sharkey, P. J. Loll, *Biochemistry* **2001**, *40*, 5172–5180.
[42] E. D. Thuresson, M. G. Malkowski, K. M. Lakkides, C. J. Rieke, A. M. Mulichak, S. L. Ginell, R. M. Garavito, W. L. Smith, *J. Biol. Chem.* **2001**, *276*, 10358–10365.
[43] M. G. Malkowski, E. D. Thuresson, K. M. Lakkides, C. J. Rieke, R. Micielli, W. L. Smith, R. M. Garavito, *J. Biol. Chem.* **2001**, *276*, 37547–37555.
[44] K. Gupta, B. S. Selinsky, C. J. Kaub, A. K. Katz, P. J. Loll, *J. Mol. Biol.* **2004**, *335*, 503–518.
[45] C. A. Harman, C. J. Rieke, R. M. Garavito, W. L. Smith, *J. Biol. Chem.* **2004**, *279*, 42929–42935.
[46] K. Gupta, B. S. Selinsky, P. J. Loll, *Acta Crystallogr. Sect. D Biol. Crystallogr.* **2006**, *62*, 151–156.
[47] C. A. Harman, M. V. Turman, K. R. Kozak, L. J. Marnett, W. L. Smith, R. M. Garavito, *J. Biol. Chem.* **2007**, *282*, 28096–28105.
[48] G. Rimon, R. S. Sidhu, D. A. Lauver, J. Y. Lee, N. P. Sharma, C. Yuan, R. A. Frieler, R. C. Trievel, B. R. Lucchesi, W. L. Smith, *Proc. Natl. Acad. Sci.* **2010**, *107*, 28–33.
[49] R. S. Sidhu, J. Y. Lee, C. Yuan, W. L. Smith, *Biochemistry* **2010**, *49*, 7069–7079.
[50] S. Xu, D. J. Hermanson, S. Banerjee, K. Ghebreselasie, G. M. Clayton, R. M. Garavito, L. J. Marnett, *J. Biol. Chem.* **2014**, *289*, 6799–6808.
[51] J. R. Kiefer, J. L. Pawlitz, K. T. Moreland, R. A. Stegeman, W. F. Hood, L. J. Marnett, J. K. Gierse, A. M. Stevens, D. C. Goodwin, S. W. Rowlinson, et al., *Nature* **2002**, *405*, 97–101.
[52] S. W. Rowlinson, J. R. Kiefer, J. J. Prusakiewicz, J. L. Pawlitz, K. R. Kozak, A. S. Kalgutkar, W. C. Stallings, R. G. Kurumbail, L. J. Marnett, *J. Biol. Chem.* **2003**, *278*, 45763–45769.
[53] J. L. Wang, D. Limburg, M. J. Graneto, J. Springer, J. R. B. Hamper, S. Liao, J. L. Pawlitz, R. G. Kurumbail, T. Maziasz, J. J. Talley, et al., *Bioorganic Med. Chem. Lett.* **2010**, *20*, 7159–7163.
[54] K. C. Duggan, M. J. Walters, J. Musee, J. M. Harp, J. R. Kiefer, J. A. Oates, L. J. Marnett, *J. Biol. Chem.* **2010**, *285*, 34950–34959.
[55] A. J. Vecchio, M. G. Malkowski, *J. Biol. Chem.* **2011**, *286*, 20736–20745.
[56] K. C. Duggan, D. J. Hermanson, J. Musee, J. J. Prusakiewicz, J. L. Schneib, B. D. Carter, S. Banerjee, J. A. Oates, L. J. Marnett, *Nat. Chem. Bio.* **2011**, *7*, 803–809.
[57] A. J. Vecchio, B. J. Orlando, R. Nandagiri, M. G. Malkowski, *J. Biol. Chem.* **2012**, *287*, 24619–24630.
[58] M. A. Windsor, D. J. Hermanson, P. J. Kingsley, S. Xu, B. C. Crews, W. Ho, C. M. Keenan, S. Banerjee, K. A. Sharkey, L. J. Marnett, *ACS Med. Chem. Lett.* **2012**, *3*, 759–763.
[59] M. J. Uddin, B. C. Crews, S. Xu, K. Ghebreselasie, C. K. Daniel, P. J. Kingsley, S. Banerjee, L. J. Marnett, *ACS Chem. Biol.* **2016**, *11*, 3052–3060.
[60] M. A. Windsor, P. L. Valk, S. Xu, S. Banerjee, L. J. Marnett, *Bioorganic Med. Chem. Lett.* **2013**, *23*, 5860–5864.
[61] B. J. Orlando, M. J. Lucido, M. G. Malkowski, *J. Struct. Biol.* **2015**, *189*, 62–66.
[62] A. L. Blobaum, S. Xu, S. W. Rowlinson, K. C. Duggan, S. Banerjee, S. N. Kudalkar, W. R. Birmingham, K. Ghebreselasie, L. J. Marnett, *J. Biol. Chem.* **2015**, *290*, 12793–12803.
[63] S. N. Kudalkar, S. P. Nikas, P. J. Kingsley, S. Xu, J. J. Galligan, C. A. Rouzer, S. Banerjee, L. Ji, M. R. Eno, A. Makriyannis, et al., *J. Biol. Chem.* **2015**, *290*, 7897–7909.
[64] W. Neumann, S. Xu, M. B. Sárosi, M. S. Scholz, B. C. Crews, K. Ghebreselasie, S. Banerjee, L. J. Marnett, E. Hey-Hawkins, *ChemMedChem* **2016**, *11*, 175–178.
[65] M. J. Lucido, B. J. Orlando, A. J. Vecchio, M. G. Malkowski, *Biochemistry* **2016**, *55*, 1226–1238.
[66] B. J. Orlando, M. G. Malkowski, *J. Biol. Chem.* **2016**, *291*, 15069–15081.

[67] M. C. Goodman, S. Xu, C. A. Rouzer, S. Banerjee, K. Ghebreselasie, M. Migliore, D. Piomelli, L. J. Marnett, *J. Biol. Chem.* **2018**, *293*, 3028–3038.
[68] S. Xu, M. J. J. Uddin, S. Banerjee, L. J. L. J. Marnett, M. Jashim Uddin, S. Banerjee, K. Duggan, J. Musee, J. R. Kiefer, K. Ghebreselasie, et al., *J. Biol. Chem.* **2019**, *294*, 8690–8689.